International
WOCE
Newsletter

Number 36 ISSN 1029-1725 September 1999

IN THIS ISSUE

News from the WOCE IPO

W. John Gould, Director, WOCE IPO and ICPO, Southampton Oceanography Centre, UK. john.gould@soc.soton.ac.uk

Summer in Kiel

Well I finally made it to my first WOCE AIMS-phase Workshop on the North Atlantic in Kiel. As we expected, this was a popular workshop with 150 people registered of whom about half were from Germany.

The workshop was a mix of plenary talks (30 in all), poster sessions (75 posters). All aspects of N. Atlantic WOCE science were covered but it seemed a pity that the results from the large scale deployments of floats were not reported. Maybe it is too early.

The discussions around the posters were lively and long (lubricated by beer one day and fortified by cake on another) and I am sure that many new collaborations will have been stimulated. There were four working group discussions on the topics of "North Atlantic synthesis products", "Mechanisms of decadal variability", "Improved parameterisations for large scale models" and "Requirements for future observations". These sessions were perhaps less successful than we had hoped (maybe there were just too many people). However, while the formal report of the workshop has yet to be completed there was agreement on the need to better understand and parameterise dense overflows, on the fact that even over the densely observed N. Atlantic there are discrepancies between oceanic and air-sea flux estimates that cannot yet be satisfactorily explained, and a perception that we still need to learn how to use all aspects of float data in the validation of models. Needless to say there was strong endorsement for the continuation of all types of N. Atlantic observations so as to better define seasonal and decadal variability.

About WOCE

The World Ocean Circulation Experiment (WOCE) is a component of the World Climate Research Programme (WCRP), which was established by WMO and ICSU, and is carried out in association with IOC and SCOR.

WOCE is an unprecedented effort by scientists from more than 30 nations to study the large-scale circulation of the ocean. In addition to global observations furnished by satellites, conventional in-situ physical and chemical observations have been made in order to obtain a basic description of the physical properties and circulation of the global ocean during a limited period.

The field phase of the project lasted from 1990–1997 and is now being followed by Analysis, Interpretation, Modelling and Synthesis activities. This, the AIMS phase of WOCE, will continue to the year 2002.

The information gathered during WOCE will provide the data necessary to make major improvements in the accuracy of numerical models of ocean circulation. As these models improve, they will enhance coupled models of the ocean/atmosphere circulation to better simulate – and perhaps ultimately predict – how the ocean and the atmosphere together cause global climate change over long periods.

WOCE is supporting regional experiments, the knowledge from which should improve circulation models, and it is exploring design criteria for long-term ocean observing system.

The scientific planning and development of WOCE is under the guidance of the Scientific Steering Group for WOCE, assisted by the WOCE International Project Office (WOCE IPO):

- W. John Gould, *Director*
- Peter M. Saunders, *Staff Scientist*
- N. Penny Holliday, *Project Scientist*
- Roberta Boscolo, *Project Scientist*
- Sheelagh Collyer, *Publication Assistant*
- Jean C. Haynes, *Administrative Assistant*

For more information please visit:
http://www.soc.soton.ac.uk/OTHERS/woceipo/ipo.html

From the WOCE IPO (continued)

I would like to take this opportunity to thank Fritz Schott, the members of the science and local organising committees and all the people who made the workshop run so smoothly. The next WOCE Newsletter in December will focus on N. Atlantic science.

The WOCE Conference book

It was agreed after the WOCE Conference in May 1998 that we should produce a book that would be based on the conference plenary presentations and would serve as a review of where the science of WOCE stands at the end of the 20th century. The book is being edited by John Church and Gerold Siedler and will be published by Academic Press. I am pleased to say that the majority of the chapters are now undergoing review and I hope that in the next Newsletter we will be able to advertise the book and you will be able to order your copy.

Meetings to come

October is a busy month. The WOCE Scientific Steering Group will meet at Scripps and will be reviewing the progress that WOCE is making towards its objectives, how we should publicise these achievements and deciding on the actions that the SSG and IPO need to take to help this process along. We will also be considering whether further workshops would be useful. At present we have scheduled on variability and representativeness in Japan in late 2000 and global fluxes workshop in 2001. We will also be discussing the plans for a final WOCE Conference in 2002.

Later in October will be the OceanObs99 conference in St. Raphael in France. It will be making the case for sustained ocean observations for climate and a number of position papers assessing the likely contribution from various observational methods will be presented. Over the past weeks I have been working with John Toole and others to do this for deep sea hydrography and have been encouraged to see the sustained level of interest in this activity from many countries.

And finally ...

"Therefore the study of the climates of the sea involves a knowledge of its currents both cold and warm. They are the channels through which the waters circulate, and by means of which the harmonies of old ocean are preserved". Matthew Fontaine Maury "The Physical Geography of the Sea", 1855.

Was this the earliest presentation of the case for doing WOCE?

The CLIPPER Project: High Resolution Modelling of the Atlantic

A.-M. Treguier, T. Reynaud and T. Pichevin, Laboratoire de Physique des Océans, IFREMER, Brest; B. Barnier, J.-M. Molines, A. P. de Miranda, C. Messager and J. O. Beismann, Laboratoire des Ecoulements Geophysiques et Industriels, CNRS, Grenoble; G. Madec, N. Grima and M. Imbard, Laboratoire d'Océanographie Dynamique et de Climatologie, CNRS, Paris; C. Le Provost, Laboratoire d'Etudes en Géophysique et Océanographie Spatiale, Toulouse, France. treguier@ifremer.fr

The contribution of France to the WOCE field programme has been concentrated in the Equatorial and South Atlantic Ocean. As a contribution to WOCE-AIMS (Analysis, Interpretation, Modelling and Synthesis), the CLIPPER project helps the interpretation of observations by carrying out model simulations of the Atlantic Ocean Circulation, either forced by air-sea fluxes or coupled with an atmospheric model. The project team will perform experiments with a prognostic, high-resolution primitive equation model (Mercator grid with resolution of 1/6° at the equator, over the whole Atlantic basin). A high resolution model is needed because of the high resolution of the WOCE data, the emphasis of the observations on the western and eastern boundaries of the South Atlantic (regions where narrow currents are found), and because of the large number of Lagrangian float observations. A second objective of CLIPPER is to help understand the role of local processes or features (such as mesoscale eddies, boundary currents, bottom topography) in shaping the ocean circulation at basin scale and driving its variability and its interactions with the atmosphere.

Beyond the technical aspects of a community, high-resolution modelling effort, CLIPPER is expected to generate original projects gathering observationalists, modellers, and theoreticians with the objective of investigating important scientific issues.

Model configurations

The CLIPPER numerical experiments are carried out by a project team, made of scientists and engineers from 4 laboratories (LEGI in Grenoble, LPO in Brest, LODYC in Paris, LEGOS in Toulouse). Four different model configurations (Table 1) are based on the same primitive equation parallel code OPA 8.1 (Madec et al., 1998). The ATL3 configuration runs on a T3E machine on 52 processors; the ATL6 configuration requires 140 processors. The model is initialised using the Atlantic Ocean climatology especially developed by Reynaud et al. (1998) for the project.

The purpose of the ATL1 configuration is to test the forcing fields and open boundaries at low cost. The NATL configuration is very similar to the configurations used in the E.U. DYNAMO project (the DYNAMO Group, 1997). Its robustness and the simplicity of closed boundaries make it attractive for the implementation of assimilation methods.

The ATL3 configuration has been run for 15 years with a climatological forcing (average of the ECMWF reanalysis, years 79–93) in order to test the full model domain with an eddy permitting resolution. Preliminary results of this experiment are presented here. The 1/6° experiment is now under way.

Open boundaries

The model has open boundaries at Drake Passage and south of Africa (30°E). The open boundary algorithm is a combination of radiation (Orlanski type) and relaxation to climatology. It is based on the South Atlantic model of Barnier et al. (1998). In the latter model, the baroclinic velocities at the boundary were calculated from the climatology by geostrophy and a simple analytic form was assumed for the barotropic streamfunction.

Preliminary experiments with the ATL1 configuration have shown a great sensitivity of the model solution to the arbitrary profile at Drake Passage. When the barotropic flow is concentrated to the north of the passage as in Barnier et al. (1998), the heat transport at 30°S is large (0.6 PW), but the barotropic flow east of Drake passage is marked by a strong meander to the south which is not realistic. When the barotropic flow in the passage is distributed over a wider latitude band, the local circulation is more realistic

Table 1. The CLIPPER model configurations

	Name	Boundaries	Number of points	Grid size
Low Resolution (1°) Atlantic	ATL1	lon: 98.5° W to 30° E; lat: 75S to 70° N	131 x 218, 42 levels	min: 28 km, max: 111 km
Middle Resolution (1/3°) Atlantic	ATL3	lon: 98.5° W to 30° E; lat: 75° S to 70° N	417 x 649, 42 levels	min: 9.6 km, max: 37 km
North Atlantic (1/3°)	NATL	lon: 98.5° W to 20° E; lat: 20° S to 70° N	358 x 361, 42 levels	min: 12.6 km, max: 37 km
High Resolution (1/6°) Atlantic	ATL6	lon: 98.5° W to 30° E; lat: 75° S to 70° N	733 x 1296, 42 levels	min: 4.8 km, max: 18.5 km

but the heat transport at 30°S is reduced by a factor of two (0.3 PW). The influence of the changes at the Drake passage propagates into the model domain as a coastal Kelvin wave along Argentina. It is not sure that higher resolution configurations would display the same sensitivity to the profile of the barotropic streamfunction, because high amplitude boundary currents should likely prevent the propagation of the Kelvin wave.

This study led us to propose a less arbitrary method to determine the barotropic velocities at Drake. It is based on the assumption of "equivalent barotropic" dynamics, which is confirmed by models and observations in the Antarctic Circumpolar Current (Killworth, 1992). With that hypothesis the currents are in phase over the vertical and the barotropic velocities can be estimated using a reference level at the bottom. Two different estimates of the barotropic velocities obtained in this manner using the climatology of Reynaud et al. (1998) and the WOCE synoptic section A21 (Roether et al., 1993) are presented in Fig. 1. The total transports are 82 and 112 Sv, respectively. The ACC frontal system appears smoothed out in the climatology. We decided to use the synoptic section on the hypothesis that the frontal structure is important to force an eddy resolving model. The final barotropic velocities used on the simulations have been calculated by smoothing the synoptic profile of Fig. 1 to remove the recirculations, and rescaling to reach a volume transport across the passage of 140 Sv.

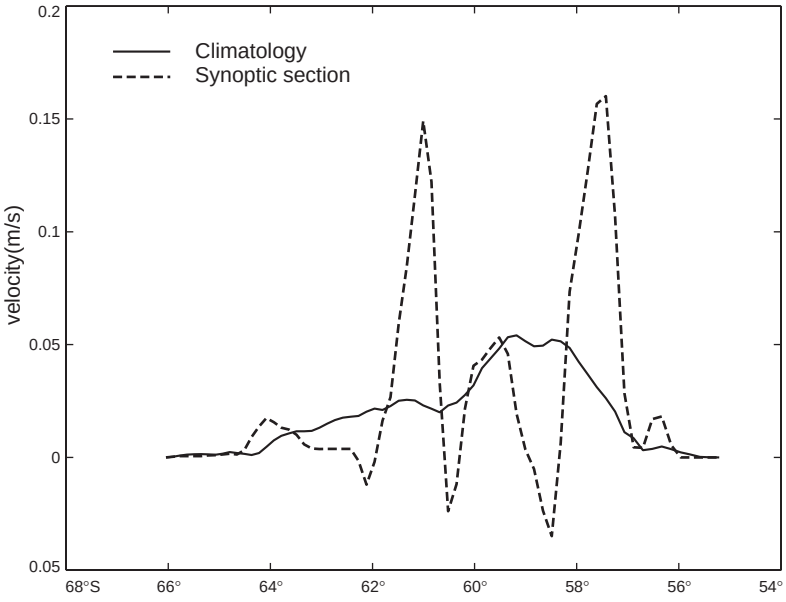

Figure 1. Barotropic velocity (geostrophic calculation referenced to the bottom) obtained with the climatology of Reynaud et al. (1998) and the WOCE section A21 (Roether et al., 1993).

A similar calculation is performed at the eastern boundary at 30°E, based on the WOCE section I6 (Park et al., 1998).

ATL3 experiment driven with ECMWF re-analysis climatology

The first experiment was run for 15 years with a climatological forcing (the average of the ECMWF reanalysis wind and fluxes). Preliminary results are described in a report available on the CLIPPER web site (www.ifremer.fr/lpo/clipper).

The time averaged barotropic streamfunction is represented in Fig. 2. The path of the ACC and its frontal structure are well represented, as well as the Agulhas current retroflection, showing the good behaviour of the open boundaries. The Brazil-Malvinas confluence zone is situated too far south at 45°S. This may be a phenomenon similar to the wrong position of the Gulf Stream separation in the North Atlantic, a problem due to inadequate resolution and lack of inertia.

In the North Atlantic, the ATL3 experiment has many similarities with the "z-coordinates" KMDM model (The DYNAMO Group, 1997). For example, ATL3 has the same heat transport at 25°N (0.9 PW) and the meridional overturning cell has a similar strength (nearly 14 Sv). Note that ATL3 uses the same buffer-zone conditions north of the sills as that used by the DYNAMO models, which is another confirmation of the DYNAMO findings that at this resolution the overturning is greatly determined by the overflows. An important difference comes from the representation of the Mediterranean Sea. The Strait of Gibraltar is closed in KMDM, but is open in ATL3 with a locally refined grid (a 10 km grid size in the strait). The Mediterranean outflow is 0.8 Sv at the strait and increases downstream by entrainment. This clearly produces an enhancement of the Azores current. It confirms the hypothesis of Jia (1999) about the influence of the Mediterranean Waters on the dynamics of the Azores front. However, the model Mediterranean outflow is much too shallow in the Gulf of Cadiz, and additional parameterisation is certainly required to make it reach the right depth.

In the South Atlantic, production of Agulhas eddies is very regular, with a frequency of 3.5 per year over 10 years of simulation. This behaviour is similar to the one observed in the POP5 global ocean model with a similar grid size (0.28° at the Equator, Maltrud et al., 1998). It is interesting to note that the generation of Agulhas rings was very irregular in the 1/3° South Atlantic simulations performed with a Sigma coordinate model by de Miranda (1996) or Béranger (1999, personal communication), suggesting that the topography is likely to influence the generating process. However, the number of eddies is also of the order of 3.5 per year.

Conclusion

The CLIPPER project has set up a series of model configurations in the Atlantic at various resolutions. These configurations should allow to carry out series of

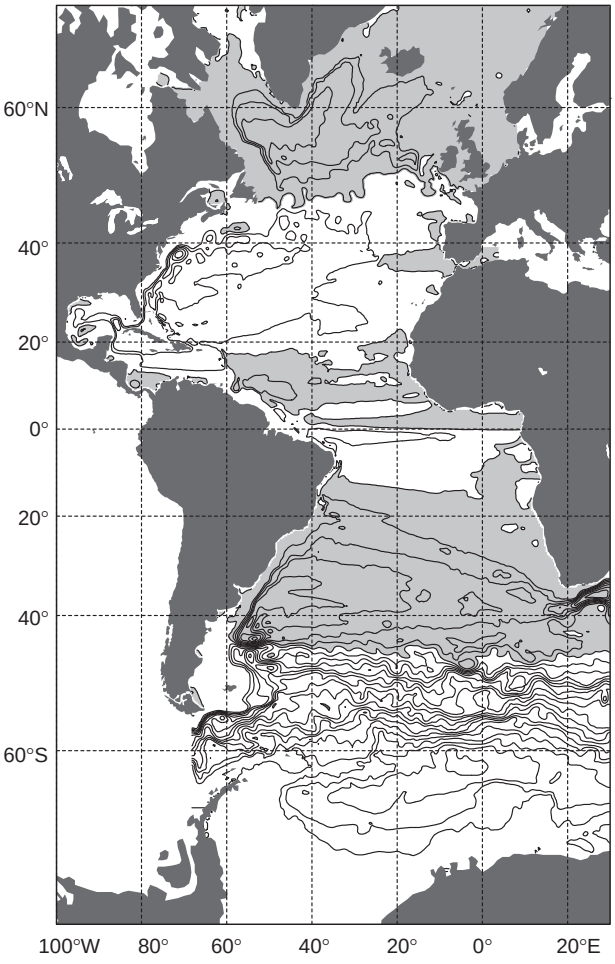

Figure 2. Barotropic streamfunction averaged over the last 5 years of the ATL3 climatological experiment. Contour interval is 10 Sv, negative contours are shaded.

experiments to investigate a wide range of topics, from the impact of the model resolution to climate changes in the Atlantic Ocean. The preliminary results of the project have already convinced us that open boundaries are a powerful approach to basin scale modelling.

The project has made a significant effort to involve the whole WOCE-France community from the beginning, to make sure that the simulations which will be carried out respond to the needs of observationalists, theoreticians and modellers involved in WOCE AIMS. Already, this approach has proven to be very useful for the definition and tuning of the various model configurations, parameterisations, initialisation and forcing fields.

The major experiment of the project is a 1/6° (Mercator grid) resolution and the model integration is presently underway. The WOCE years are being simulated with daily forcing from ECMWF re-analysis over the period 1979 to 1993. There are plans to continue this simulation up to 1998, and to carry out in a near future an experiment driven the 40 years of NCEP/NCAR re-analysis in the context of studying climate changes in the Atlantic.

Acknowledgements

The CLIPPER project acknowledges the support received from CNRS/INSU, IFREMER, SHOM and CNES.

References

Barnier, B., P. Marchesiello, A. Pimenta de Miranda, J. M. Molines, and M. Coulibaly, 1998: A sigma-coordinate primitive equation model for studying the circulation in the South Atlantic. Part I: Model configuration with error estimates. Deep-Sea Res., 45, 543–572.

De Miranda, A., 1996: Application d'un modèle numérique de circulation générale océanique permettant la génération de turbulence de méso-échelle à l'étude de l'Atlantique Sud. Thèse de l'Université J. Fourier, Grenoble.

Dynamo Group (S. Barnard, B. Barnier, A. Beckman, C. W. Böning, M. Coulibaly, B. DeCuevas, J. Dengg, C. Dieterich, U. Ernst, P. Herrmann, Y. Jia, P. D. Killworth, J. Kroeger, M.-M. Lee, C. Le Provost, J.-M. Molines, A. L. New, A. Oschlies, T. Reynaud, L. J. West, and J. Willebrand), 1997: DYNAMO: Dynamics of North Atlantic Models: Simulation and assimilation with high resolution models. Berichte aus dem Institut für Meereskunde an der Christian-Albrechts-Universitat Kiel, 294. 334 pp.

Jia, Y., 1999: On the formation of an Azores current due to Mediterranean overflow in a modelling study of the North Atlantic. J. Phys.Oceanogr., in press.

Killworth, P. D., 1992: An Equivalent-barotropic mode in the fine Resolution Antarctic Model. J. Phys. Oceanogr., 22, 1379–1387.

Madec, G., P. Delecluse, M. Imbard, and C. Levy, 1998: OPA 8.1 general circulation model reference manual. Notes de l'IPSL No. 11, 91 pp, Université P. et M. Curie, Paris Cedex 5, France.

Maltrud, M. E., R. D. Smith, A. J. Semtner, and R. C. Malone, 1998: Global eddy-resolving ocean simulations driven by 1985-1995 atmospheric winds. J. Geophys. Res., 103, 30825–30853.

Park, Y. H., and E. Charriaud, 1997: Hydrography and baroclinic transport between Africa and Antarctica on WHP section I6. Int. WOCE Newsl., 29, 13–16.

Reynaud, T., P. Legrand, H. Mercier, and B. Barnier, 1998: A new analysis of hydrographic data in the Atlantic and its application to an inverse modelling study. Int. WOCE Newsl., 32, 29–31.

Roether, W., R. Schlitzer, A. Putzka, P. Beining, K. Bulsiewicz, G. Rohardt, and F. Delahoyde, 1993: A chlorofluoromethane and hydrographic section across Drake Passage: Deep water ventilation and meridional property transport. J. Geophys. Res., 98, 14423–14435.

Potential Vorticity as a Tracer in Quantitative Water Mass Analysis

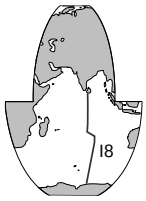

Matthias Tomczak, FIAMS, Flinders University, Australia.
matthias.tomczak@flinders.edu.au

The hydrographic data set collected during WOCE provides an excellent basis for a quantitative census of the world ocean's water masses. Various efforts are already under way in this direction. Several of these studies are not based on temperature and salinity only but make use of water mass indicators such as nutrients, the CFCs, oxygen isotopes and other tracers.

The mathematical tools for water mass analysis are evolving as well. Optimum Multiparameter (OMP) analysis began as a simple extension of the classical temperature-salinity (T/S) triangle technique; it is now used not only to derive quantitative estimates of water mass distributions but to determine water mass ages as well (Karstensen and Tomczak, 1998).

Most water mass analysis is based on the assumption that mixing in the ocean is fully turbulent. While allowance is made for bio-geochemical processes and, where appropriate, for natural decay, physical mixing acts on all properties in the same way. This allows us to formulate the quantitative mixing problem as a "bucket problem": Given two buckets of water, with volumes v_1 and v_2 and water properties p_1 and p_2, what will the property of the mixture be if we pour the contents of both buckets into a container of volume $v_1 + v_2$? This approach has been quite successful; but it leaves the dynamical oceanographer somewhat dissatisfied, since it ignores some powerful and well known dynamical constraints that determine which particles can come into contact with each other when the two buckets are emptied and which particles cannot mix.

Most of the oceanic circulation is in geostrophic equilibrium. A well-known property of a layer of thickness H in such a flow field is the potential vorticity $pv = (\zeta + f) / H$, which is conserved along particle paths, ($\zeta = \partial v / \partial x - \partial u / \partial y$ is the relative vorticity; f is the planetary vorticity or Coriolis parameter). In most parts of the world ocean, and in particular in the interior of the large subtropical and subpolar gyres, ζ is always much smaller than f, and the conservation theorem for potential vorticity can then be written as $pv = f / H$ = constant. For a continuously stratified ocean this theorem takes the form $pv = fN^2 / g$, where $N = (g / \rho \, \partial\rho / \partial z)^{1/2}$ is the Brunt-Väisälä frequency, ρ density and g the acceleration of gravity. This is a quantity which can be derived from hydrographic station data and can therefore be included in ordinary water mass analysis.

This note reports some preliminary results of a first attempt to include potential vorticity in the "bucket mixing" scheme of OMP analysis. Its aim is to test the feasibility of using potential vorticity as a standard tracer along with the classical tracers temperature, salinity, oxygen and nutrients.

Methods and data

OMP analysis has become a standard tool in oceanography and requires only a brief introduction. A more detailed summary can be found in Poole and Tomczak (in press), among others. The web site of the OMP User Group (Karstensen and Tomczak, 1999) also contains a description of the method.

In a nutshell, OMP analysis defines water masses by source water types in n-dimensional parameter space, where n is the number of observational parameters (Tomczak, 1999). It includes the condition of mass conservation to solve the linear system of equations

$$\mathbf{A\,x - d = R}$$

where **A** is the source water type matrix, **d** is the vector of observational data for one water sample, **x** is the solution vector (the contributions of the water masses which make up the water sample) and **R** is a vector of residuals. The last row of A expresses the condition of mass conservation. The system is solved subject to a non-negativity constraint which excludes negative water mass contributions. All parameters are normalised before the analysis is applied and weighed. The weights are determined from the source water types and from the observations; they are proportional to the spread of the source water types and inversely proportional to the scatter of observations taken in the water mass formation regions. Because the system is solved by minimising the residuals, the number of source water types included in the analysis cannot exceed the number of observational parameters.

The data for this note come from WOCE hydrographic section I8 in the Indian Ocean and include all stations between the equator and 30°S. Section I8 was planned to extend along 80°E through both hemispheres, but for reasons explained below only data from the southern hemisphere are included here. South of 25°S the section angles away in a south-eastward direction, to end at about 88°S.

Only bottle data were used in this preliminary study. The WOCE station network generally has better depth coverage than earlier hydrographic sections, with a sampling interval of 100 m or less above the 1000 m level (the maximum analysed depth level for this study). Potential vorticity was calculated by linear differentiation of the bottle data density, which was derived from bottle temperature and salinity. For comparison, potential vorticity was also calculated from CTD data. Because the calculation involves a vertical differentiation, the calculation from a

high-resolution data set such as CTD data produces a very noisy depth profile for potential vorticity and requires some form of depth filtering. A moving average over at least a 40 m depth interval is the minimum treatment required with CTD data. Comparison between potential vorticity profiles derived from filtered CTD data with those derived from bottle data showed no significant differences between both profiles.

The data were used in an OMP analysis based on temperature, salinity, oxygen, phosphate, nitrate and silicate with six water types representing four water masses, Indian Central Water (ICW), Australasian Mediterranean Water (AAMW, representing the Indonesian Throughflow), Antarctic Intermediate Water (AAIW) and Indian Equatorial Water (IEW). Source water type definitions for temperature, salinity, oxygen and nutrients to define these water masses in their formation regions can be found in the literature. The present study requires also source water type definitions for potential vorticity. They were derived from potential temperature–potential vorticity diagrams of the I8 data and represent local conditions not necessarily representative for conditions in the water mass formation regions. To make all definitions consistent, all source water types used in this study were also derived from local property–property diagrams.

Table 1 shows the definitions used. Weights for temperature, salinity, oxygen and nutrients are based on Karstensen (1999). The weight for potential vorticity was originally calculated in the same manner as weights for the other parameters, but the elevated scatter which results from the differentiation with depth makes the weight unrealistically low (lower than all nutrient weights). It should be noted that, in a way, the choice of the weight for potential vorticity relative to the weights of all other parameters represents the user's trust in geostrophy. The present preliminary study is based on a "neutral approach" which gives potential vorticity the same weight as the other conservative properties.

Because the source water types are locally defined all parameters, the effects of water mass ageing can be considered negligible in comparison to advection and mixing. Redfield ratios were therefore not used in this study, and OMP analysis was applied in its basic form (see the OMP User Group (Karstensen and Tomczak, 1999) for details).

Results

Fig. 1 shows the water mass distribution derived from basic OMP analysis without the use of potential vorticity. As expected, Indian Central Water dominates the thermocline, which rises towards the equator. It is bound at depth by the Antarctic Intermediate Water, which at 13°S (1450 km) contributes some 20% to the water at 600 m depth. Closer to the equator its place is taken up by Indian Equatorial Water, a water mass produced by subsurface mixing in the western equatorial Indian Ocean and by double diffusion along its return flow towards east with the strong zonal currents along the equator (Karstensen, 1999). Australasian Mediterranean Water only contributes to the water mass structure in the upper thermocline of the equatorial region. The distribution resembles closely the one derived by Karstensen (1999) and is in good agreement with the generally accepted situation in the south-eastern Indian Ocean.

In assessing the quality of the analysis it is useful to look at distributions of residuals in space. The mass conservation residual is particularly instructive, since mass should be conserved during the mixing process. The bottom left panel of Fig. 1 shows the residual for mass conservation for the OMP analysis without the use of potential vorticity. The residual is less than 1% over most of the section, indicating a reliable result, but there are regions where the residual is unacceptably high. One such region is located at the upper depth limit of the analysis, where the residual reaches values in excess of 30%. The boundary between acceptable values and unacceptably large residuals is quite sharp and coincides with the density level $\sigma_t = 26.0$ (compare the bottom right panel) and the isotherm $\Theta = 17.8°C$, which is the highest temperature defined for ICW (Table 1). Observed temperatures above $\Theta = 17.8°C$ in a region of nearly pure ICW can only be accommodated with the selected source water types if negative water mass

Table 1: Source water type definitions, weights and Redfield ratios used in this study

water mass	potential temperature (° C)	salinity	oxygen (µmol kg^{-1})	PO_4 (µmol kg^{-1})	NO_3 (µmol kg^{-1})	Si (µmol kg^{-1})	mass conserv.	potential vorticity (10^8 s^{-1} m^{-1})
Upper ICW	17.8	35.9	200	0.0	0	0.5	1	0.4
Lower ICW	10.0	34.8	240	1.05	14.4	5	1	0.005
Upper AAMW	17.8	34.7	66	1.3	12	14	1	0.01
Lower AAMW	10.0	34.7	66	2.0	30	30	1	0.005
Upper IEW	20.3	35.325	90	1.2	16	12	1	0.0
Lower IEW	7.0	34.97	45	2.75	36.5	74	1	0.0
AAIW	4.87	34.418	180	2.1	31	38	1	0.2
Weights	24	24	7	2	2	2	24	24

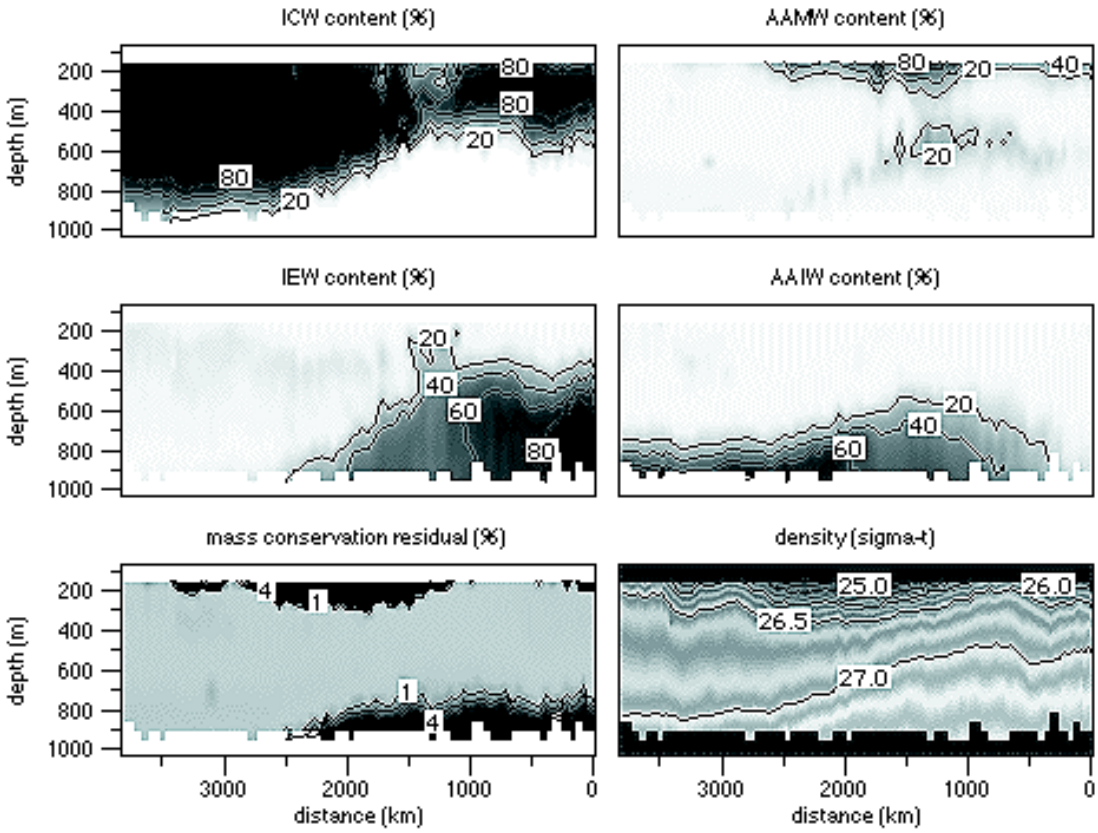

Figure 1. Water mass distribution along WOCE section I8 between the equator and 30°S, derived from OMP analysis based on temperature, salinity, oxygen and nutrients. The horizontal scale shows distance from the equator. From the equator to 24°S (2664 km) the section runs along 80°E, the remainder runs south eastward to reach 88.5°E at the end of the section shown. The bottom panels show the residual of mass conservation and density (σ_t).

contributions are accepted. The large errors of the mass conservation residual in the upper thermocline are therefore the result of the non-negativity constraint.

A second region of large mass conservation residuals is found below the thermocline. The deterioration of the solution with depth is more gradual here, and the maximum residual does not exceed 10%. The boundary coincides roughly with the density level $\sigma_t = 27.25$ between ICW and AAIW. The gradual increase of the residual suggests that the reason for the deterioration of the solution is to be found in inaccuracies in the source water type definitions.

The mass conservation residual restricts the validity of the result to the permanent thermocline between $\sigma_t = 26.0$ and $\sigma_t = 27.25$. While this makes the calculated AAIW contribution for the section somewhat irrelevant, the fact that mixing of AAIW into the lower thermocline does occur is shown by the 20% AAIW contour which is well within the region of acceptable mass conservation residuals.

Fig. 2 shows the results of basic OMP analysis when potential vorticity is included as a tracer. The general arrangement of the water masses remains the same (compared to the analysis without potential vorticity) but there are some significant differences. The decrease of ICW content in the thermocline core from nearly 100% to less than 80% is coupled with a corresponding increase of IEW content. This is clearly a spurious result, since IEW cannot occur at such distance from the equator without a clearly defined propagation path to link it to its equatorial source region. The disappearance of ICW north of 5°S (555 km) is due to an increased presence of both IEW and AAMW. This region is close to the spreading paths of both water masses, and the changed result cannot be discarded without further study.

A look at the mass conservation residual (bottom left of Fig. 2) shows that all regions where significant changes in the water mass distribution are observed have to be regarded as regions where the analysis is unreliable. The region of acceptable mass conservation residuals (<1%, taken from Fig. 2) is considerably reduced. The residual of potential vorticity (bottom right) shows a very similar distribution and reinforces the fact that the solution which includes potential vorticity gives only an acceptable representation of the water mass distribution over a limited range of the thermocline.

Discussion

The analysis shows that potential vorticity can be included in OMP analysis as an additional tracer at least for a limited density range. The question arises whether the reduction in the range of acceptable mass conservation residuals is a

consequence of ocean dynamics (as expressed by the conservation of potential vorticity) or a shortfall of the method. It is generally true that regions of unacceptably high residuals are regions of high residuals for all parameters. The absolute values of the residuals of a particular parameter can be controlled by an appropriate choice of its weight, but the relative distribution of the residuals remains unchanged. The narrowing of the acceptable range of the solution when potential vorticity is included is therefore independent of the weight allocation to potential vorticity. Experiments with different weights ranging from 2 (the weight given to the nutrients) to 100 (an arbitrary increase to give potential vorticity more prominence) showed that the basic character of the solution remains unchanged. Inclusion of potential vorticity in the analysis produces an unrealistic reduction of ICW content in the central thermocline and the disappearance of ICW from the equatorial region.

Our knowledge of the water mass distribution in the Indian Ocean thermocline is sufficiently well established to allow us to say that the changes produced by including potential vorticity are most likely physically unrealistic. Two explanations offer themselves. Either the concept of conservation of potential vorticity does not apply to this part of the Indian Ocean, or the source water type definitions for potential vorticity require amendment. The first possibility is unlikely, at least for the centre of the subtropical gyre where potential vorticity is well described by fN^2 / g. The situation near the equator is questionable, since the basic assumption which underlies the calculation of potential vorticity is not valid at the equator. It is interesting to note that the region of acceptable potential vorticity residuals does extend into the equator at 600–800 m depth, suggesting that the failure of the solution near the equator is not necessarily a result of equatorial dynamics.

In a wider context, how a water mass crosses the equator and maintains its potential vorticity is an unresolved issue. As a water particle approaches the equator its potential vorticity begins to be dominated by the relative vorticity of the flow field. The layer thickness H of the thermocline can get very small at the equator, but there comes a point where the eventual disappearance of f in $pv = (\zeta + f) / H$ at the equator can no longer be compensated by a decrease of H. Away from the western boundary, the only term in $\zeta = \partial v / \partial x - \partial u / \partial y$ which can make up for the disappearance of f is $\partial v / \partial x$. This leads to a rapid increase of zonal flows as the equator is approached. Intense zonal currents at the equator have been described by various authors, for example Luyten and Swallow (1976). At the western boundary $\partial u / \partial y$ can become important, allowing the water mass to cross the equator. This pathway has been documented for ICW by You and Tomczak (1993) and Karstensen (1999), but it cannot explain what happens to its

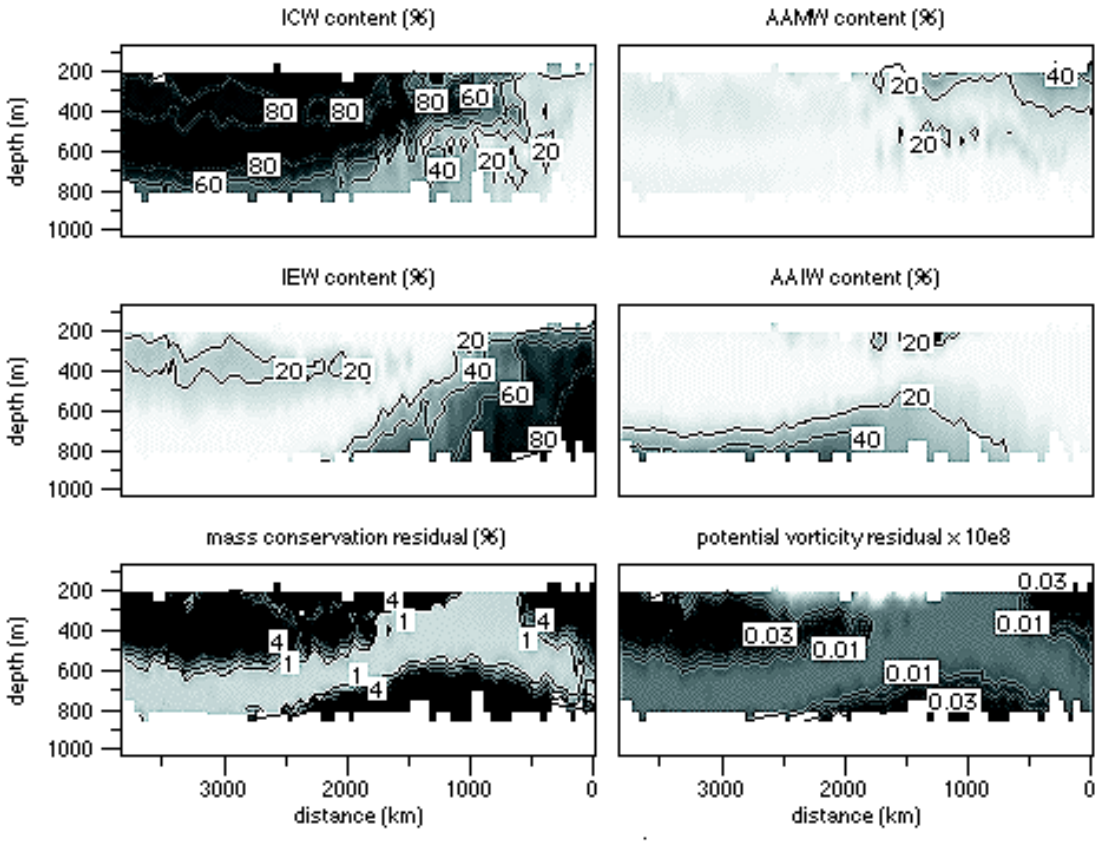

Figure 2. Water mass distribution along the section shown in Figure 1, derived from OMP analysis based on the same parameters and, in addition, potential vorticity. The bottom panels show the residuals of mass conservation (%) and potential vorticity (10^8 s^{-1} m^{-1}).

potential vorticity when it spreads through the northern Indian Ocean. The stratification in the permanent thermocline is essentially the same in both hemispheres, so the Brunt-Väisälä frequency in the depth range of ICW remains about the same, but its potential vorticity $pv = (fN^2 / g)$ changes sign. Nof and Borisov (1998) discussed this problem for Bottom Water and invoke frictional (bottom and slope) mixing. Whether this is applicable to all water depth remains unclear.

Irrespective of these complications at the equator it seems clear that the major reason for the discrepancies between the OMP solution with and without the use of potential vorticity arise mainly from inadequate source water type definitions for potential vorticity. Determining potential vorticity in water mass formation regions is a major requirement for future applications, which will have to be based on extended OMP analysis which includes the effects of water mass ageing. The very least which this can achieve is that one more tracer is available for OMP analysis, allowing the inclusion of one additional source water type. This may turn out to be less of a gain than it sounds, since there are indications that potential vorticity is not a linear function of potential temperature in the thermocline. Proper modelling of ICW may therefore require more than two source water types before the spurious minimum in the central thermocline is eliminated. The degree of freedom gained by including potential vorticity may therefore be lost by the need for an additional set of source water types.

There are of course other reasons why potential vorticity should be included. If OMP analysis is applied to data on surfaces it will become possible to derive mass fluxes and mixing rates across particle paths as functions of space (and ultimately time, as the data density increases). Such a study is planned for the Indian Ocean. The preliminary exploratory work described here gives reason to expect that it will produce a reliable result.

The Matlab code for the latest version of OMP analysis, which includes potential vorticity as a water mass tracer, can be downloaded from the OMP User Group web site (Karstensen and Tomczak, 1999). The site also offers an online user guide with detailed instructions and an example of an application.

References

Karstensen, J., 1999: Über die Ventilation the Thermocline des Indischen Ozeans. PhD thesis, University of Hamburg.

Karstensen, J., and M. Tomczak, 1998: Age determination of mixed water masses using CFC and oxygen data. J. Geophys. Res., 103, 18599–18610.

Karstensen, J., and M. Tomczak, 1999: OMP analysis version 2.0. OMP User Group web site, http://www.ifm.uni-hamburg.de/~wwwro/omp_std/omp_std.html

Luyten, J. R., and J. C. Swallow, 1976: Equatorial undercurrents. Deep-Sea Res., 23, 999–1001.

Nof, D., and S. Borisov, 1998: Inter-hemispheric oceanic exchange. Q. J. R. Meteorol. Soc., 124, 2829–2866.

Poole, M., and M. Tomczak, 1999: Optimum multiparameter analysis of the water mass structure in the Atlantic Ocean thermocline. Deep-Sea Res., in press.

Tomczak, M., 1999: Some historical, theoretical and applied aspects of quantitative water mass analysis. J. Mar. Res., 57, 275–303.

You, Y. and M. Tomczak, 1993: Thermocline circulation and ventilation in the Indian Ocean derived from water mass analysis. Deep-Sea Res., 40, 13–56.

Global Water Mass Analysis, a Symposium of IAPSO at the IUGG General Assembly

Matthias Tomczak, FIAMS, Flinders University, Australia. matthias.tomczak@flinders.edu.au

One of the obvious applications of the WOCE data set is a quantitative analysis of the global water masses. This task is receiving growing attention and was the topic for a one day IAPSO symposium at the IUGG General Assembly in Birmingham, which was held from 19 to 30 July 1999. Forty authors from 6 countries presented 19 papers during the symposium, which was held on Monday 19 July, the first day of the two-week meeting. Presentations covered processes of water mass formation, water mass climatology, water masses in ocean and coupled ocean/atmosphere models, and regional water mass studies. Between 20 and 30 people attended the symposium at various stages during the day.

The initiative for the symposium goes back to a successful water mass workshop which was held at the previous IAPSO meeting in Melbourne during July 1997. That workshop, which was initially planned as a meeting of experts with short invited presentations and plenty of discussion time, was eventually attended by more than 50 people. The workshop drew on members from three communities: physical oceanographers, tracer oceanographers and ocean modellers. The success of the workshop encouraged IAPSO to include a water mass symposium in its programme for 1999.

Another related event was the WOCE Tracer Workshop held in Bremen in February this year. It attracted over

Table 1. Parameters used for water mass analysis in the presentations to the Global Water Mass Analysis symposium at IUGG, Birmingham								
	temperature	salinity	oxygen	nutrients (silicate)	CFCs	tritium	helium	artificial tracers
Number of papers	14	13	3	3 (2)	1	1	1	1

70 participants, mainly from the tracer and modelling community. Physical oceanography was represented by a few conspicuous individuals, but the balance between the three groups was not as even as it had been in Melbourne two years earlier. This was of course understandable, given the focus of the workshop on the present and future of tracer oceanography.

Compared to these previous events the symposium in Birmingham seemed to be of more modest proportions, but this does not reflect a decrease of interest in the topic. The somewhat smaller attendance was partly due to a plethora of parallel sessions, partly due to the absence of many tracer oceanographers, who had their own session, "Stable Isotopes and Trace Substances: their Use in Oceanography and Climate Research on Various Timescales", two days later. As a result the symposium was attended mainly by physical oceanographers and ocean modellers; tracer oceanographers were seen to come and go and listen to selected presentations.

The true extent of activity and interest in global water mass analysis is probably better assessed if the two sessions, Global Water Mass Analysis and Stable Isotopes and Trace Substances, are seen as a unit. Both symposia attracted between 20 and 30 people, with significant attendance overlap between the two events. (A third symposium, "Biogeochemical Constraints In The Ocean – Controls, Modelling And Prediction", was also relevant to water mass theory and analysis in some aspects, for example in the determination of accurate Redfield ratios.)

The breadth of themes covered in both symposia was a good representation of the status of water mass analysis today, ranging from new applications of traditional temperature-salinity analysis to innovative uses of new tracers in combination with old and purpose-built new methods. In this respect the Global Water Mass symposium probably represented the "traditional" end of the spectrum, with several contributions based exclusively on temperature-salinity analysis techniques. Table 1 shows the range of water mass indicators considered by the 19 papers presented. Oxygen was used in studies of water mass formation and climatology. Silicate was the preferred nutrient; 2 of the 3 studies which made use of nutrient data strongly concentrated on this parameter. One presentation of a global model study employed an artificial tracer to identify water masses.

Table 2 summarises the thematical breakdown of the presentations. Six papers concentrated on physical mechanisms of water mass formations and appropriate analysis methods, discussing aspects such as subduction rates, diapycnal vs. isopycnal mixing, and the combination of potential vorticity with other tracers. Three papers reported on global distributions or changes in water mass properties on decadal time scales. This aspect of water mass research will clearly become more prominent as the observational data base will develop during CLIVAR. Eight numerical modelling papers used water mass analysis to assess the quality of climate models, deduce water mass formation processes in inverse models and quantify water mass transformation processes. Two papers addressed details of regional water mass formation in the Tasman Sea and in the Strait of Sicily.

Table 2. Distribution of presentations over the four themes of the symposium	
theme	number of papers
formation processes	6
climatology (decadal variability)	3 (2)
modelling	8
regional studies	2

Although the symposium did not exude the same feeling of innovation and excitement which characterised the 1997 IAPSO workshop or the determination to set new goals found at the WOCE Tracer Workshop, it reinforced expectations that major advances in water mass analysis are imminent in all areas of activity. This is particularly true for the areas of methods for water mass analysis, which are evolving rapidly, and for observational studies of climatological variability. Our knowledge of the global distribution of water masses, their formation processes, formation regions and pathways is also advancing rapidly. Modellers have come to recognise that property–property plots are a more stringent test of model performance than the comparison of parameter fields in space and are looking at water masses to control model performance. It is to be hoped that the oceanographic community will maintain the close contact between physical oceanographers, tracer oceanographers and numerical modellers which developed over recent years and that future water mass symposia will continue to reflect this interaction.

Absolute Geostrophic Velocity within the Subantarctic Front in the Pacific Ocean

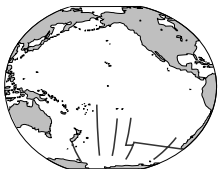

Kathleen Donohue, Eric Firing, and Shuiming Chen, University of Hawaii, USA.
kathyd@soest.hawaii.edu

In the absence of direct velocity measurements, geostrophic velocities within the Antarctic Circumpolar Current (ACC) are generally referenced to the bottom. A natural question arises: Is the bottom reference appropriate? Results from the Fine Resolution Antarctic Model (FRAM) show the tendency for the velocity to behave in an equivalent-barotropic mode; near-bottom velocities are reduced in magnitude but remain in the same direction relative to the surface velocities (Killworth, 1992). Instantaneous snapshots of the FRAM velocity field show that eastward velocity within the ACC jets extends throughout the water column (Webb et al., 1991). Recently, Heywood et al. (1999) referenced geostrophic velocities with a shipboard acoustic Doppler profiler (SADCP) and found that eastward velocities within the Southern ACC front and the Southern Boundary of the ACC extend throughout the water column. In this note we present the results of referencing geostrophic velocities to the SADCP along six WOCE Hydrographic Programme lines that crossed the ACC in the Pacific Ocean (Fig. 1, page 19). We show results only from the vicinity of the Subantarctic Front (SAF), where problems of data quality and ageostrophic velocity contributions were minimal. The SADCP-referenced geostrophic velocities indicate that a bottom reference underestimates the eastward flow associated with the SAF. Lowered acoustic Doppler profiles (LADCP) that sampled the SAF along one survey confirm the SADCP result there.

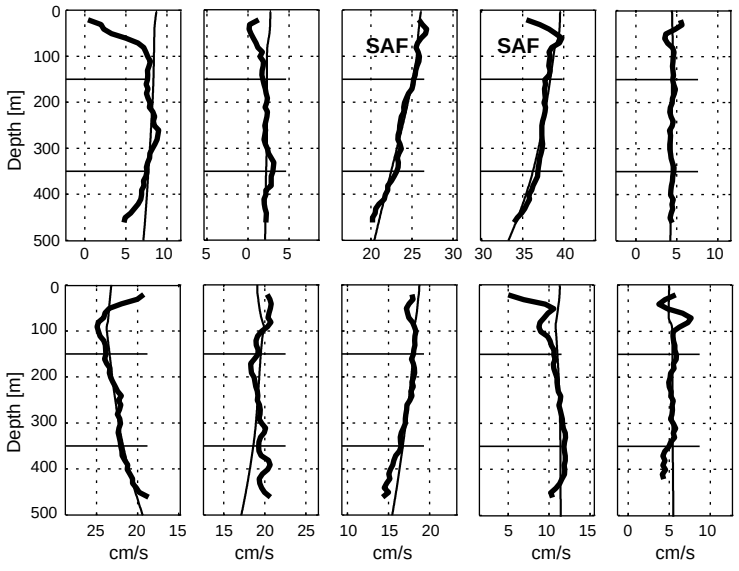

Figure 2. Comparison between the SADCP-referenced geostrophic (thin line) velocity and average SADCP cross-track velocity (thick line) for the ten station pairs near the SAF along P19. The reference depth interval is delimited by the horizontal lines.

SADCP-reference technique

The geostrophic velocity is referenced to the SADCP by matching the integrated geostrophic shear to the cross-track SADCP velocity. In the horizontal, we average between stations; in the vertical we average over the thickest layer for which the SADCP are consistently available and which avoids the surface layer where near-inertial energy is usually highest. Here, we average from 150 m to 350 m except in the few cases the SADCP velocity did not extend this deep. The bottom velocity is defined as the offset between the geostrophic velocity referenced to the SADCP and the geostrophic velocity referenced to the bottom.

Errors in SADCP reference

Errors in the SADCP reference derive mainly from two sources: instrument error and ageostrophic motion. The major contributors to the SADCP-measured ageostrophic motion are assumed to be barotropic tides, internal tides (typically dominated by the semidiurnal constituents) and near-inertial oscillations.

Instrument Error: High-accuracy GPS position and heading measurements became standard during the WHP. For the six lines, we assume that the error (1σ) in the between-station SADCP average is 1 cm/s.

Barotropic tide: The barotropic tide is removed from the SADCP using the OSU TOPEX/ POSEIDON Cross-over Global Inverse Solution, Version 3.1 (Egbert et al., 1994). The predicted barotropic tide is less than 1 cm/s for these WHP lines except near Campbell Plateau, where the predicted tide exceeds 3 cm/s.

Internal tides and near-inertial motion: An accurate estimate of the ageostrophic signal due to the internal tide and near-inertial oscillations requires a time series longer than the period of these signals; unfortunately, the typical hydrographic station sampling period is too short (3–4 hours). But if we suppose that near-inertial oscillations and semi-diurnal tide are the dominant contributors of temporal change on station and that they have different vertical structures, then we can take advantage of the tendency for near-inertial oscillations in the upper ocean to vary rapidly in the vertical, while the dominant internal tide has a relatively low modal structure. This method, developed by Firing et al. (1998), decomposes the SADCP velocity vector into two parts: a low frequency, low wavenumber (internal tide) component and a high wavenumber and/or high frequency (near-inertial) component. This

method is crude, but averaged over groups of adjacent stations, it appears to work. For the sections used here, these ageostrophic errors (1σ) range from 1.2 to 2.8 cm/s for the internal tide and from 1.4 to 2.8 cm/s for the near-inertial signal.

The combined errors (instrument and ageostrophic) are statistically independent of one another so the total uncertainty is the root sum of squares of the contributions. The between-station SADCP error (1σ) for the six lines ranges from 2.4 to 3.7 cm/s.

Curvature correction: A correction must be made when the momentum balance includes inertial terms. In regions of strong curvature, such as eddies, the flow is in gradient-wind balance rather than geostrophic balance. In order to match the SADCP to the geostrophic shear in regions of strong curvature, we make an adjustment to the SADCP velocity. The shallow absolute geostrophic velocity is calculated from the SADCP using the gradient-wind balance before the geostrophic shears are referenced. This requires an estimate of the radius of curvature from the SADCP velocity vectors in a manner similar to Saunders and King, 1995.

SADCP-referenced SAF

The SADCP instruments errors are small for these lines (1 cm/s), yet this does not ensure that the SADCP reference will be meaningful. The success of the SADCP reference relies on the assumption that the measured upper-ocean velocity is dominated by the geostrophic signal, and ageostrophic contamination of the reference is small. The comparison between the geostrophic shear and the between-station cross-track SADCP velocity profile provides an indication of the high wavenumber small vertical scale ageostrophic noise in the SADCP. The comparison for the station pairs along the six lines is favourable. (Results for P19 are shown in Fig. 2.) The r.m.s. of the difference between the SADCP and SADCP-referenced geostrophic velocity over the reference depth interval ranges from 0.1 to 1.4 cm/s, indicating that ageostrophic noise is minimal and that the reference velocity is not sensitive to the choice of reference depth range.

The results of the SADCP reference applied to the SAF regions are presented in Fig. 3 (page 19). Rather then examining the details of the individual lines, several general features are highlighted. First, SADCP velocity vectors distinguish jets associated with the SAF from adjacent eddies. Second, strong bottom (3 cm/s) velocities can be found in the eddies. See, for example, the small anticyclonic eddy near 56°S along P15. The curvature correction applied to eddies for the six lines is less than 2.5 cm/s except for a small intense cyclone near 56°S adjacent to the SAF along P17. The inferred bottom velocity for the station pair 76,77 changes from 4.2 cm/s westward to 3.6 cm/s eastward. Finally, bottom velocities are eastward within the SAF, ranging from 4 cm/s to 10 cm/s.

Details for the SADCP reference are provided for P15, which had concurrent LADCP measurements (Fig. 1). The most striking features are two eddies bracketing the SAF, an anticyclone to the north and a cyclone to the south (Fig. 3). The velocity vectors show the resulting strong convergence into the SAF. Another anticyclonic eddy is found in the southern portion of P15 near 56.3°S. The bottom reference yields eastward transport for four station pairs surrounding the SAF with peak transport at the SAF. The SADCP reference shows strong eastward bottom velocities near the SAF. The strongest eastward bottom velocity is located at the northern SAF station pair (7.9 ±2.5 cm/s). The curvature adjustment has been applied to the three eddies. The adjustment is less than 1 cm/s except for station pair 59,60 where it decreases the eastward bottom velocity from 9.8 cm/s to 7.9 cm/s.

Contours of LADCP velocity for the SAF region along P15 support the conclusion from the SADCP

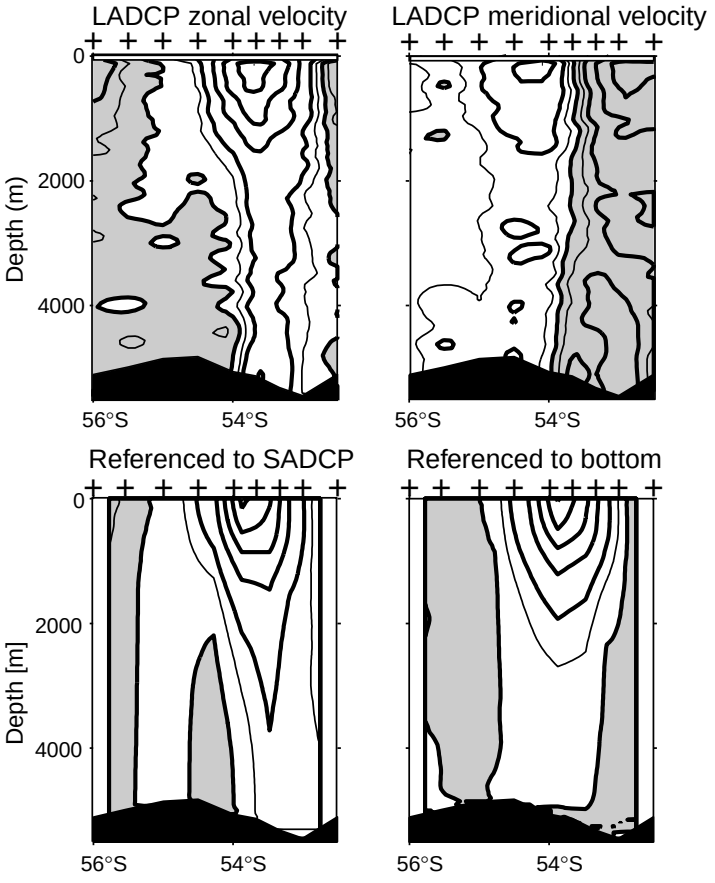

Figure 4. The LADCP zonal velocities (upper left) show that the eastward flow associated with the SAF extends throughout the water column. This compares favourably with the SADCP-referenced geostrophic velocities (lower left) and illustrates that the bottom reference (lower right) misses this eastward bottom flow. The LADCP meridional velocities (upper right) also show the deep penetration of the surface flows and reveal that the convergence into the SAF extends throughout the water column. LADCP data are de-tided. Westward and southward velocities are grey-shaded. The main contour interval is 10 cm/s, with the thin contours at ±5 cm/s.

reference: zonal velocities associated with the SAF extend throughout the water column (Fig. 4). Similar to the SADCP reference, the strongest near-bottom velocities are shifted to the north relative to the near-surface maximum. Below about 2000 m, the zonal velocity within the SAF is nearly uniform with depth and maximum speeds are about 12 cm/s (station 59, 53.67°S). The meridional velocities also show the deep penetration of the surface flows and the convergence into the SAF extending throughout the water column.

Discussion and conclusions

The SADCP-referenced geostrophic velocities indicate that a bottom reference underestimates the eastward flow within the SAF. Bottom velocities range from 4 cm/s to 10 cm/s. LADCP velocities confirm this result along P15. The SADCP-referenced geostrophic velocities show that the spatial structure of the bottom velocities across the SAF is not smooth; bottom velocities can change by as much as 12 cm/s over 50 km.

An accurate representation of the reference level velocities may not be necessary to accurately determine property fluxes across hydrographic sections. McIntosh and Rintoul (1997) explored the performance of several inverse models using output from FRAM. They find that when interfacial fluxes are included as unknowns and column weights are chosen correctly, the property fluxes are accurate even though the resulting reference level velocities are smoothly varying and poorly resolve the actual reference level velocities in the FRAM output. McIntosh and Rintoul (1997) state that "The successful flux estimates reflect the fact that the variability of the reference level velocity on small spatial scales does not carry a significant net flux of heat or salt".

Unlike the net property fluxes, the fundamental dynamical balances of the ACC cannot be determined without an accurate representation of the velocity field. In particular, the eastward flow beneath the Drake Passage sill depth must recirculate on local and/or gyre scales. The nature of these deep recirculations warrants further investigation.

Future work will focus on evaluating the dynamics in the POP-11 model which accurately represents ACC transport at Drake Passage (Maltrud et al., 1999) and also exhibits deep-reaching ACC jets.

Acknowledgements

We thank the following principal investigators for the use of the hydrographic data from the WOCE one-time surveys. P14S and P15S: J. Bullister and G. Johnson; P16S and P17S: J. Reid; P17E and P19: J. Swift. We would also like to thank A. Orsi for providing the historical frontal locations and June Firing, Craig Huhta, and Mae Zhou for processing the SADCP and LADCP data.

References

Egbert, G. D., A. F. Bennet, and M. G. Foreman, 1994: TOPEX/POSEIDON tides estimated using a global inverse model. J. Geophys. Res., 99, 24821–24852.

Firing, E., S. Chen, K. A. Donohue, P. Hacker, and J. Hummon, 1998: Velocity field estimation from shipboard ADCP, lowered ADCP, and geostrophy. In: World Ocean Circulation Experiment Meeting, Halifax, NS, Canada.

Heywood, K., M. Sparrow, J. Brown, and R. Dickson, 1999: Frontal structure and Antarctic Bottom Water Flow through the Princess Elizabeth Trough, Antarctica. Deep-Sea Res., 46, 1181–1200.

Killworth, P. D., 1992: An equivalent-barotropic mode in FRAM. J. Phys. Oceanogr., 22, 1379–1387.

Maltrud, M. E., R. D. Smith, A. J. Semtner, and R. C. Malone, 1998: Global eddy-resolving ocean simulations driven by 1985–1995 atmospheric winds. J. Geophys. Res., 103, 30825–30844.

McCartney, M. S., 1977: Subantarctic mode water. In: A Voyage of Discovery, M. Angel (ed.), George Deacon 70th Anniversary Volume, pp. 103–119, Pergamon, New York.

McIntosh, P., and S. R. Rintoul, 1997: Do box inverse models work? J. Phys. Oceanogr., 27, 291–308.

Orsi, A. H., T. Whitworth, and W. D. Nowlin, 1995: On the meridional extent and fronts of the Antarctic Circumpolar Current. Deep-Sea Res., 42, 641–673.

Saunders, P. M., and B. A. King, 1995: Bottom currents derived from a shipborne ADCP on WOCE cruise A11 in the South Atlantic. J. Phys. Oceanogr., 25, 329–347.

Webb, D., P. D. Killworth, A. Coward, and S. R. Thompson, 1991: The FRAM atlas of the Southern Ocean. Natural Environment Research Council, Swindon, UK, 66 pp.

Introducing SOLAS (Surface Ocean Lower Atmosphere Study)

Douglas Wallace, Abt. Meereschemie, Inst. für Meereskunde an der Universität Kiel, Germany.
dwallace@ifm.uni-kiel.de

A new international research programme called SOLAS ('Surface Ocean Lower Atmosphere Study) has now entered the active planning stage. SOLAS is aiming for an improved understanding of marine and atmospheric biogeochemical processes in the context of the physical environment, including climate change. This understanding is the required foundation for assessment and prediction of changes in marine and ocean biogeochemistry that may result from global change. The study of feedbacks between ocean biogeochemistry and climate change will also be a central theme of SOLAS.

SOLAS would build on the work of several previous programmes, principally IGAC, JGOFS and WOCE, and would be closely linked to CLIVAR. Its uniqueness would be the bringing together of atmospheric and marine researchers, including representatives from the biogeochemistry, atmospheric chemistry, paleooceanographic and physical oceanography communities in order to examine the interaction between climate, atmospheric chemistry and marine biogeochemistry. Those partnerships have not been widely realised to date and in many countries they are hindered by funding structures. Such barriers to interdisciplinary science will need to be overcome if SOLAS is to succeed.

SOLAS is also envisaged as a hypothesis-driven programme in that hypotheses arising from critical issues related to global change will be posed and specific manipulative experiments and studies will be designed in order to test them. Some early suggestions of hypotheses and experiments were given in an early description of SOLAS published in the IGBP Newsletter article (A. J. Watson, 1997; Global Change Newsletter 31, pp. 9–12; see also the SOLAS web page

http://www.ifm.uni- kiel.de/ch/solas/main.html).

The Scientific Committee on Oceanic Research (SCOR) and the IGBP have sponsored the planning of SOLAS to date with considerable interest from the World Climate Research Programme (WCRP). After the scientific mission, focus and hypotheses of SOLAS are fully developed, it will be considered as a potential core project of the IGBP.

The 15-member planning committee includes representatives of several current global change research programmes. Current members are:

Jim Aiken, Plymouth Marine Laboratory, UK

Richard Barber, Duke University Marine Laboratory, US

Leonard Barrie, Atmospheric Environment Service, Canada

Robert Duce, Texas A&M University, US

Emilio Fernandez, University of Vigo, Spain

Martin Heimann, Max Planck Institut für Biogeochemie, Germany

Barry Huebert, University of Hawaii, US

Dileep Kumar, National Institute of Oceanography, Goa, India

Peter Liss, University of East Anglia, UK

Patricia Matrai, Bigelow Laboratory for Ocean Science, US

Liliane Merlivat, Université Pierre et Marie Curie, France

Peter Schlosser, Lamont-Doherty Earth Observatory, US

Mitsuo Uematsu, University of Tokyo, Japan

Douglas Wallace, Institut für Meereskunde, Kiel, Germany

Andrew Watson, University of East Anglia, UK

The committee met last December to begin planning an open science conference for SOLAS, which will be held 20–24 February 2000 (see announcement in this issue). The purpose of the conference is to bring together interested scientists to discuss and propose the scientific questions, themes and approaches that will form the basis for SOLAS. Using input from this meeting, the planning committee will develop an initial scientific blueprint or science plan for the programme. IGBP and SCOR and possibly other interested bodies such as the WCRP and the Commission on Atmospheric Chemistry and Global Pollution (CACGP) will subsequently consider this plan for implementation.

Preliminary Results of CANIGO Subproject 1.2.5: A Lagrangian Description of the Azores Current

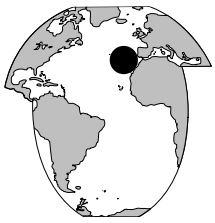

Michael Sparrow, AINCO-Interocean, Spain; Michaela Knoll, IFM Kiel and FWG, Germany; Bernd Lenz, IFM Kiel, Germany; Alán Cantos, AINCO-Interocean, Spain. mike.sparrow@ainco.es

The CANIGO project is part of the MAST-III Regional Seas Research programme and involves partners from 12 countries and 45 institutions. Its main goal is:

- To understand the functioning of the marine system in the Canary Islands–Azores–Gibraltar region of the north-east Atlantic Ocean and its links with the Alboran Sea through comprehensive interdisciplinary basin scale studies.

The project is split into four sub-projects investigating the physical, chemical and biogeochemical processes in the CANIGO area. Further details of these can be found at:

http://www.marine.ie/datacentre/projects/canigo

The objectives of this particular study are:

- To provide a Lagrangian description of the Azores Current (AC).
- To investigate the transition between the AC and the Canary Current (CC).
- To study whether the AC also feeds the poleward undercurrent along the African shelf.

The AC and the CC are part of the eastern recirculation of the North Atlantic subtropical gyre and are thus essential parts of the large-scale oceanic circulation. The AC is the extension of the south-eastern branch of the Gulf Stream that crosses the Mid-Atlantic Ridge at about 34–36°N (Klein and Siedler, 1989). Typical maximum surface velocities of the jet are $20 - 40\,\mathrm{cm\,s^{-1}}$ with transports of 10–15 Sv (where $1\mathrm{Sv} = 10^6\,\mathrm{m^3 s^{-1}}$) containing North Atlantic Central Water (Käse and Krauss, 1996).

The AC splits into three main southward recirculation branches, which later join the westward-flowing North Equatorial Current (Siedler and Onken, 1996; Tychensky et al., 1998). These branches, which vary seasonally and interannually, are found just east of the Mid-Atlantic Ridge, in the central basin near 23°W and near the coast of West Africa respectively (Stramma and Siedler, 1988). The easternmost branch of the AC is thought to feed the CC, an integral part of the Eastern Boundary Current System. While the large-scale flow pattern is known, the details of the processes by which the AC water is incorporated in the eastern boundary flow and then transported southward and westward are, however, not well understood.

Previous studies have shown evidence of westward counter-currents and recirculations close to the AC (Cromwell et al., 1995; Pingree, 1997; Alves and Colin de Verdière, 1999).

Some of the water reaching the continental slope near Morocco is thought to contribute to a poleward flowing upper layer slope flow that reaches the Iberian peninsula (Pingree, 1997).

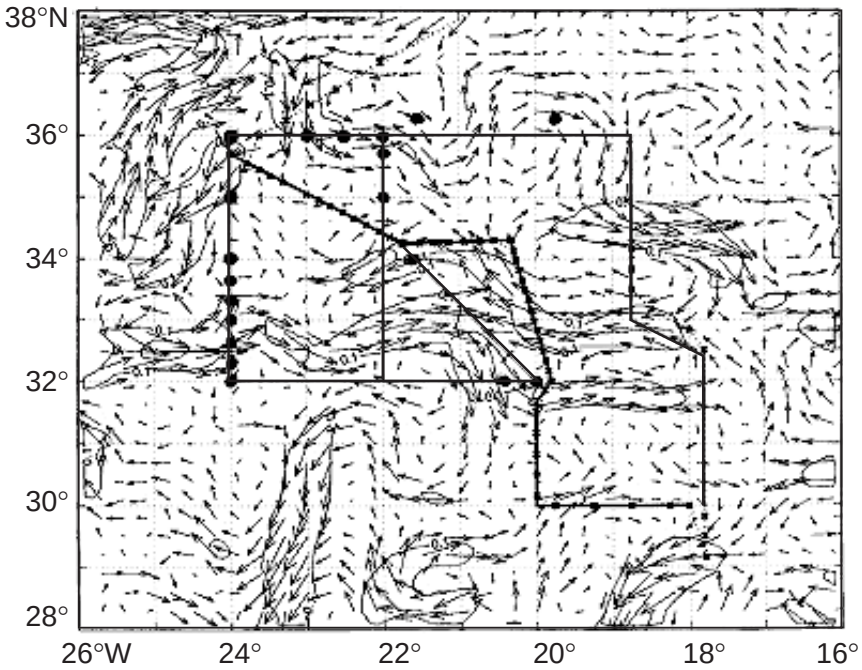

Figure 1. The streamfunction predictions of a quasi-geostrophic altimeter data assimilating model and the RAFOS float deployment positions (black dots). Part of cruise track showing area of investigation is also shown.

Data and methods

Eleven RAFOS floats from IfM Kiel and nine RAFOS floats from AINCO-Interocean were deployed south-east of the Azores during a cruise with NO Thalassa in July 1997 in the central Canary Basin. The floats were deployed on the second leg of the cruise, which started on 14 July 1997 in Santa Cruz de La Palma and ended on 1 August 1997 in Lisbon (Fig. 1).

The mission lengths of the floats were set to either 1 year or 1.5 years. The floats were ballasted for an approximate depth of 500 m, corresponding to a

density level of about $27.1\,kg/m^3$.

The RAFOS floats were tracked by triangulation of distances between the floats and moored sound sources (see, for example, Sparrow et al., 1998). Temperature and pressure were also recorded by the floats.

In order to fulfil the objectives of this study the RAFOS floats had to be launched within, or very close to, the AC. In order to position the AC accurately we examined (a) hydrographic data (CTD, ADCP, XBT and thermosalinograph results) collected during the cruise (CANIGO subtask 1.2.3) and (b) the stream function predictions of a quasi-geostrophic model based on altimeter data from CANIGO subtask 1.2.1.3 (Giraud et al., 1997).

The model results of 22 July 1997 (during the cruise), at 550 m suggest several current branches within the survey region (Fig. 1). One branch flows broadly eastward between 36–37°N and another first moves eastward at 32–33°N and then bifurcates between 20°W and 21°W. There is a strong counter-current between about 33°N and 34°N, just to the north of the southernmost branch. This clearly demonstrates the complex structure of the AC in this region.

In total the floats returned almost 16 years of data. Four of the floats failed to return any data and a few surfaced earlier than expected. Consultation with the manufacturers led to the conclusion that the early surfacing of some of the floats was the result of fish bite of the nylon cord attached to the drop weight (this problem was also encountered during the AMUSE experiment (Bower et al., 1997). The reason for the failure of the other four floats is still under investigation.

Results

The complex pattern of the AC suggested by the model results is mirrored in the paths of the floats (Fig. 2, page 20). Except for floats 426 and 432, all floats surfaced south of their launching positions, with the east-west distribution being more or less equal.

Two of the floats (422 and 423), which were released north of 34.5°N, turned eastward after initially moving northward and surfaced east of Madeira. This corresponds to the expected eastward branch of the AC, which turns southward north-east of Madeira. However, floats 430 and 432 released in the same area turned westward and surfaced considerably to the west of their launching positions. This westward motion coupled with the drop in average temperature (by 0.6°C) of float 432 (float 430 returned no temperature data) compared with the average of floats 422 and 423 could be a signal that the float moved into cooler and fresher Azores recirculated water (Cromwell et al., 1995).

Float 426 was launched within 3 minutes of an arc of float 422, in the northern branch of the AC. For the first 40 days they showed similar paths with a northward movement followed by a south-eastward motion. Instead of carrying on to the east, though, float 426 moved broadly northwestward, surfacing further north than the rest of the floats.

After about 150 days float 428 had shown little mean displacement, but after this the float was caught in the branch of the AC that flows southwards at about 23°W.

Float 427 moved in a large anti-cyclonic loop, although it was also influenced by a cyclonic circulation to the east of the Azores (also observed in the path of float 432).

Floats 418, 434, 425, 419, 429 and 420 (from north to south) were launched in a line along 24°W. Floats 418, 434, 419 and 429 moved to the east and south as would be expected of floats caught within the AC, but in a very convoluted fashion (with the exception of float 434, but this track is based on few data points). Float 425 moved south of Madeira and thereafter to the African shelf where, tantalisingly, it seems to have been caught in the CC. Although the float had surfaced it could still be tracked for a further 6 weeks until the its batteries ran out (Fig. 2). After surfacing, the float was quickly transported southwestward along the African shelf. Although its motion would have been contaminated by surface winds, it looks as if the float remained trapped in the CC during the time it was followed at the surface.

Floats 431 and 421 were captured by a branch of the AC that flowed eastward between about 32°N and 33°N. However, according to the model results this branch bifurcated at about 20–21°W, one branch continued eastward at about 32°N and another moved southward. Unfortunately, float 431 surfaced only after 6 days. Initially, float 421 seemed to have been caught within the eastward flowing branch, but after 30 or so days it escaped and moved westward.

Only the mean displacement is available for float 430. The model results indicate it was launched in the boundary between eastward and westward flow and moved in the latter direction.

The path of float 436 was very different to the rest of the floats. It showed a strong degree of anti-cyclonic motion interrupted by periods of less regular motion. Evidently the float was trapped by some kind of anti-cyclonic eddy. At this stage, from the float data alone, it is difficult to say whether the eddy was a Meddy or a Meddy-like anticyclone as observed by Richardson (1993). Examination of concurrent hydrographic data should solve this at a later date. The mean velocity of the float was $1.5 \pm 3.2\,cm\,s^{-1}$ at 221°. This is close to $0.74 \pm 0.54\,cm\,s^{-1}$ at 210° for three Meddies and $2.6 \pm 0.6\,cm\,s^{-1}$ at 253° for three anti-cyclones (Richardson, 1993) observed in the eastern basin.

The rotation period of about 6–10 days is suggestive of a Meddy when compared with, e.g. 2–7 day period for Meddies observed in AMUSE (Bower et al., 1997) rather than the (30 day period observed for the weaker form of anti-cyclones (Richardson, 1993). Towards the end of its mission the float's motion became more erratic, as the anticyclone collided, probably catastrophically, with the Cruiser Seamount. As this occurred, the float sank by 50 dbar and the surrounding temperature dropped by about 0.5°C.

Examination of all the float data demonstrates there was no statistically significant zonal mean current and the mean southward flow was only $0.4 \pm 0.2\,cm\,s^{-1}$ (uncer-

tainty as per the student-t test). None of the floats showed a connection to the poleward undercurrent along the Iberian peninsula.

Within the Canary Basin the path of the AC is highly convoluted with recirculations and counter currents at its northern and southern boundaries. Like former observations of surface drifters (Pingree, 1997, Tychensky et al., 1998, Hernandez and Le Traon, 1995) the CANIGO subsurface float tracks demonstrate a high degree of variability. Floats follow different paths even when they are launched close together. The same variability is observed in the hydrographic data set obtained during the Thalassa cruise (CANIGO subtask 1.2.3) as well as in the stream function predictions of the model from CANIGO subtask 1.2.1.3. The float data provides evidence of the connection between the AC and the CC, though this still requires further investigation.

Acknowledgements

We would like to thank the officers and crew of the NO Thalassa, particularly the chief scientist Fabienne Gaillard. We are also very grateful to Fabrice Hernandez on the ship and Sylvie Giraud at Toulouse for running the SOPRANE model and helping us to position the AC in real time.

References

Alves, M., and A. Colin de Verdière, 1999: Instability dynamics of a subtropical jet and applications to the Azores Front-Current System: Eddy driven mean flow. J. Phys. Oceanogr., 5, 837–864.

Bower, A. S., L. Armi and I. Ambar, 1997: Lagrangian Observations of Meddy formation during A Mediterranean Undercurrent Seeding Experiment. J. Phys. Oceanogr, 27, 2545–2575.

Cromwell, D, P. G. Challenor, and A. L. New, 1995: Does the Azores Current flow west at 35°N? Sigma, 17, 10–11.

Giraud, S., S. Baudel, E. Dombrowsky, and P. Bahurel, 1997: The SOPRANE project; real-time monitoring of the North-East Atlantic. In: Ocean circulation nowcast/forecast for oceanographic scientific campaigns. International Symposium Proceedings, Biarritz, France.

Hernandez, F., and P.-Y. Le Traon, 1995: Mapping mesoscale variability of the Azores Current using TOPEX/POSEIDON and ERS-1 altimetry, together with hydrographic and Lagrangian measurements. J. Geophys. Res., 100, 24995–25006.

Käse, R. H., and W. Krauss, 1996: The Gulf Stream, the North Atlantic Current, and the origin of the Azores Current. In: The Warmwatersphere of the North Atlantic Ocean, W. Krauss (ed.), pp. 291-337, Gebrueder Borntraeger, Berlin, Stuttgart.

Klein, B., and G. Siedler, 1989: On the origin of the Azores Current. J. Geophys. Res., 94, 6159–6168.

Pingree, R. D. 1997: The eastern subtropical gyre (North Atlantic): Flow rings recirculations structure and subduction. J. Mar. Biol. Ass. (UK), 77, 573–624.

Richardson, P. L., 1993: A census of eddies observed in North Atlantic SOFAR float data. Prog. Oceanogr., 31, 1–50.

Siedler, G., and R. Onken 1996: Eastern recirculation. In: The Warmwatersphere of the North Atlantic Ocean, W. Krauss (ed.), pp. 339-364, Gebrueder Borntraeger, Berlin, Stuttgart.

Sparrow, M. D., M. Menzel, V. Zervakis, and A. Cantos-Figuerola, 1998: Subsurface float tracking and processing using the ARTOA and ARPRO packages. Int. WOCE Newsl., 30, 34–36.

Stramma, L., and G. Siedler, 1988: Seasonal changes in the North Atlantic subtropical gyre. J. Geophys. Res., 93, 8111–8118.

Tychensky, A., P.-Y. Le Traon, F. Hernandez, and D. Jourdan, 1998: Large structures and temporal changes in the Azores Front during the SEMAPHORE experiment. J. Geophys. Res., 103, 25009–25027.

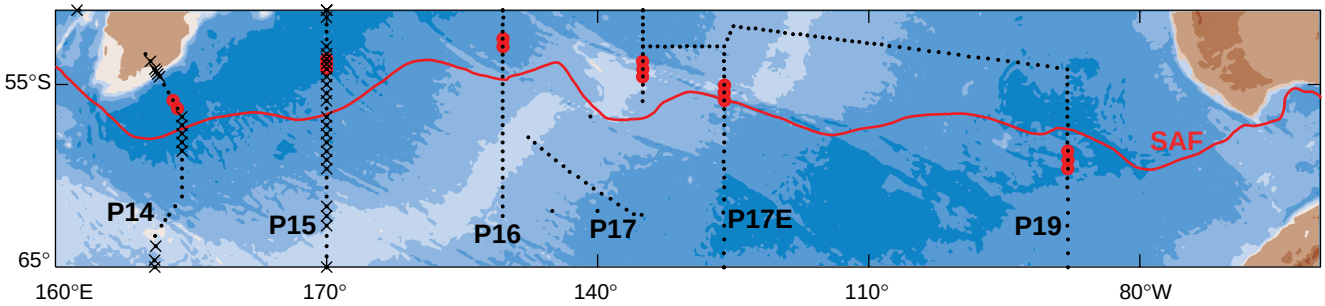

Donohue et al., page 12, *Figure 1. Positions of hydrographic stations are shown as black dots. Solid continuous red lines show the positions of the SAF determined from historical hydrographic data by Orsi et al. (1995). Using the classification from Orsi et al. (1995), we identify the SAF along the WHP lines (red dots). Briefly stated, we define the SAF as the poleward boundary of the Subantarctic Mode Water thermostad (McCartney, 1977). SADCP data are available for all lines. LADCP stations are noted by the x's. Bathymetry is shaded every 1000 m. Land is represented by the darkest brown.*

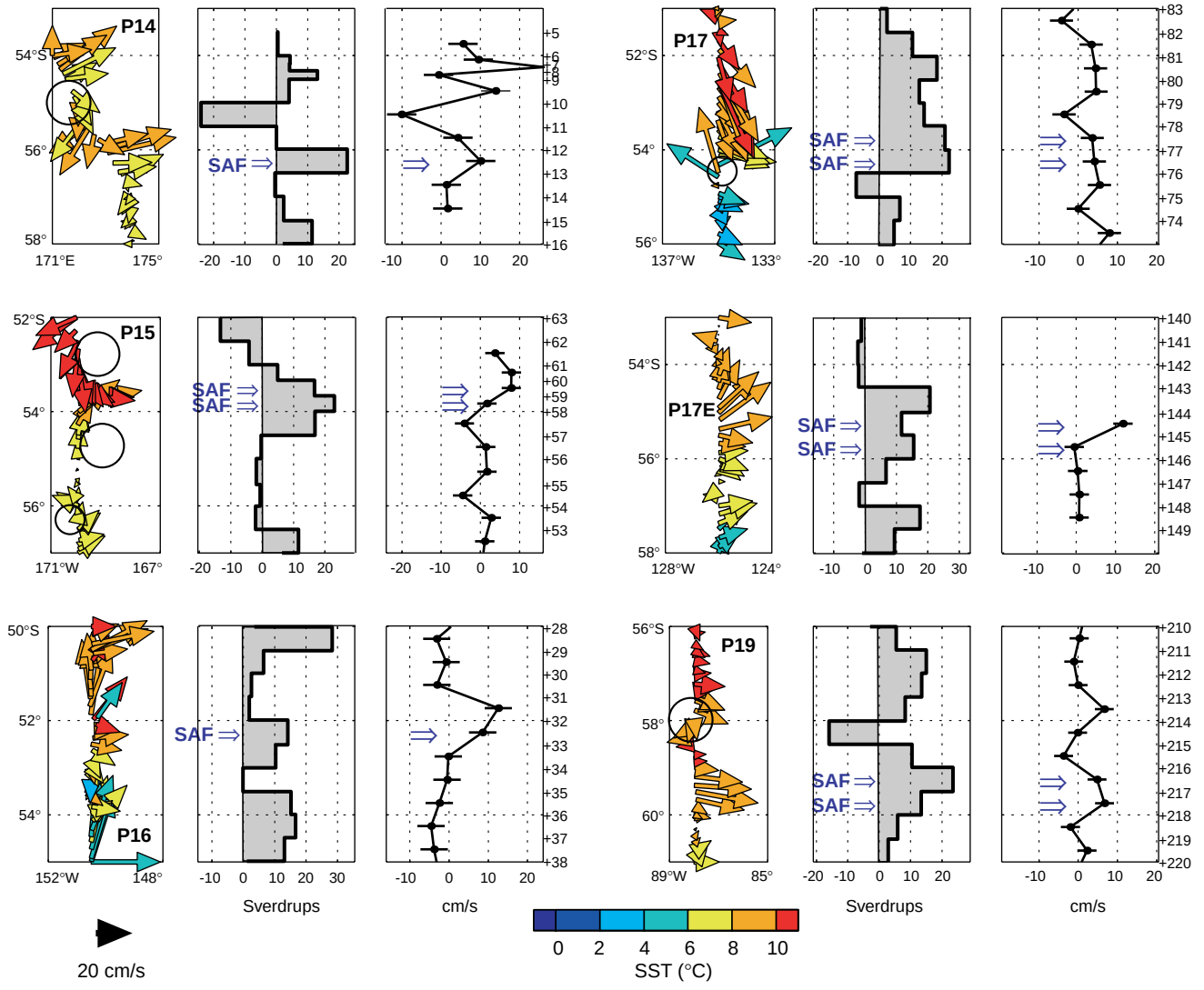

Donohue et al., page 12, *Figure 3. SADCP velocity vectors (averaged over 150–250 m and colour coded by thermistor temperature) are shown in the left panels and distinguish jets associated with the SAF from adjacent eddies (shown schematically by black circles). Between-station transports determined by referencing the geostrophic shears to zero at the deepest common level are shown in the middle panels. In the right panels, bottom velocities determined from the SADCP reference show that strong bottom (3 cm/s) velocities can be found in the eddies and that bottom velocities are eastward within the SAF. Errors (1σ) in the SADCP-reference bottom velocity are shown with horizontal lines. Positive transports and velocities are eastward. Bottom-velocity estimates are omitted on parts of P14 and P15 because of ADCP data dropouts and on P17E because of a failure of the GPS heading sensor.*

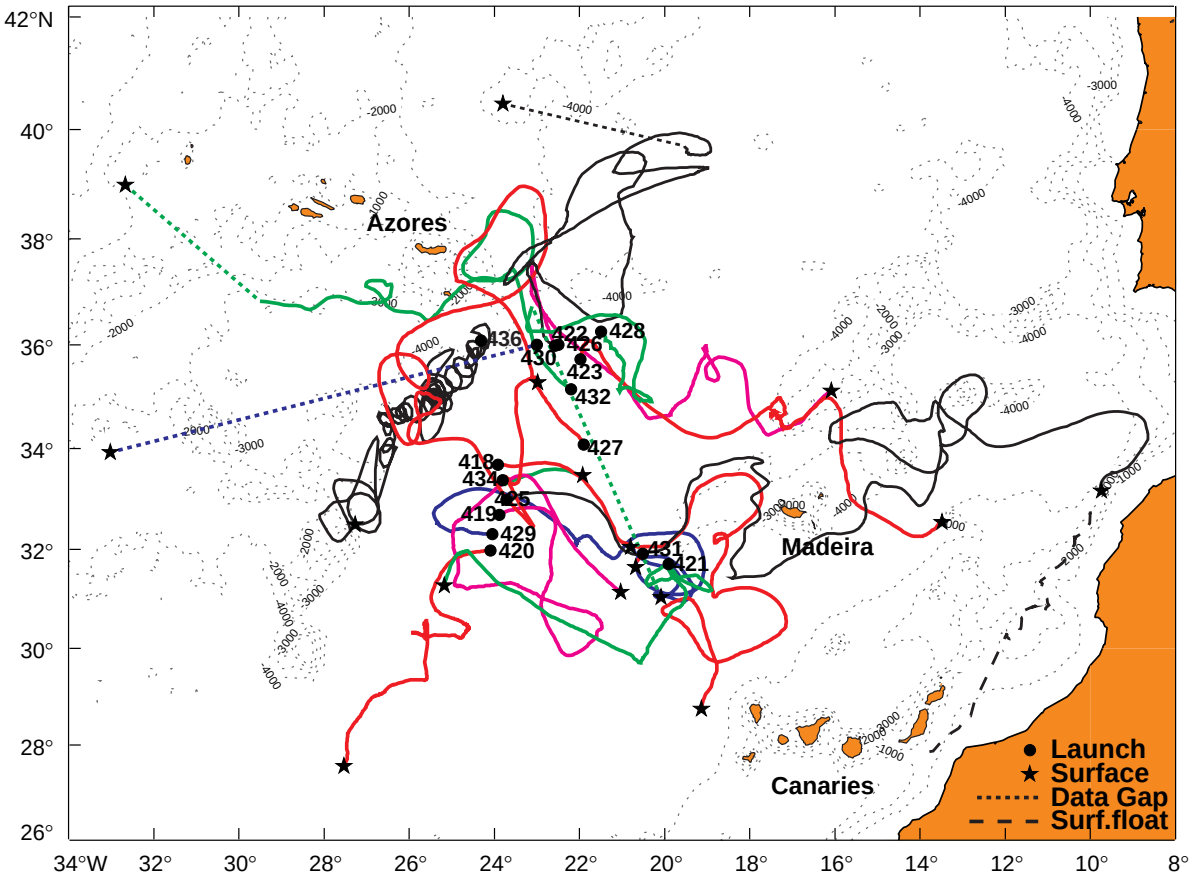

Above: Sparrow et al., page 16, *Figure 2. Float tracks showing launching positions (dots), surfacing positions (stars) and data gaps (dotted lines). Dashed line shows path of float 425 after surfacing. Also shown is bathymetry at 500 m (blue shading) and 1000 m, 2000 m, 3000 m and 4000 m depth levels.*

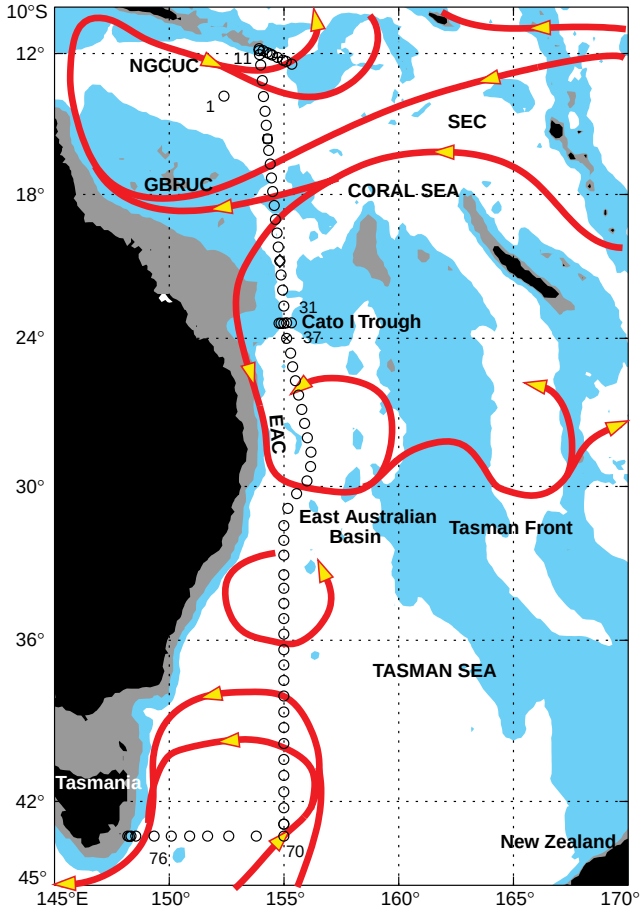

Left: Sokolov and Rintoul, page 32, *Figure 1. Position track of Franklin 9306 (WOCE section P11). Light shading indicates depth shallower than 2500 m; dark shading indicates depth shallower than 250 m. Arrows indicate major circulation features of the southwest Pacific, as described in the text.*

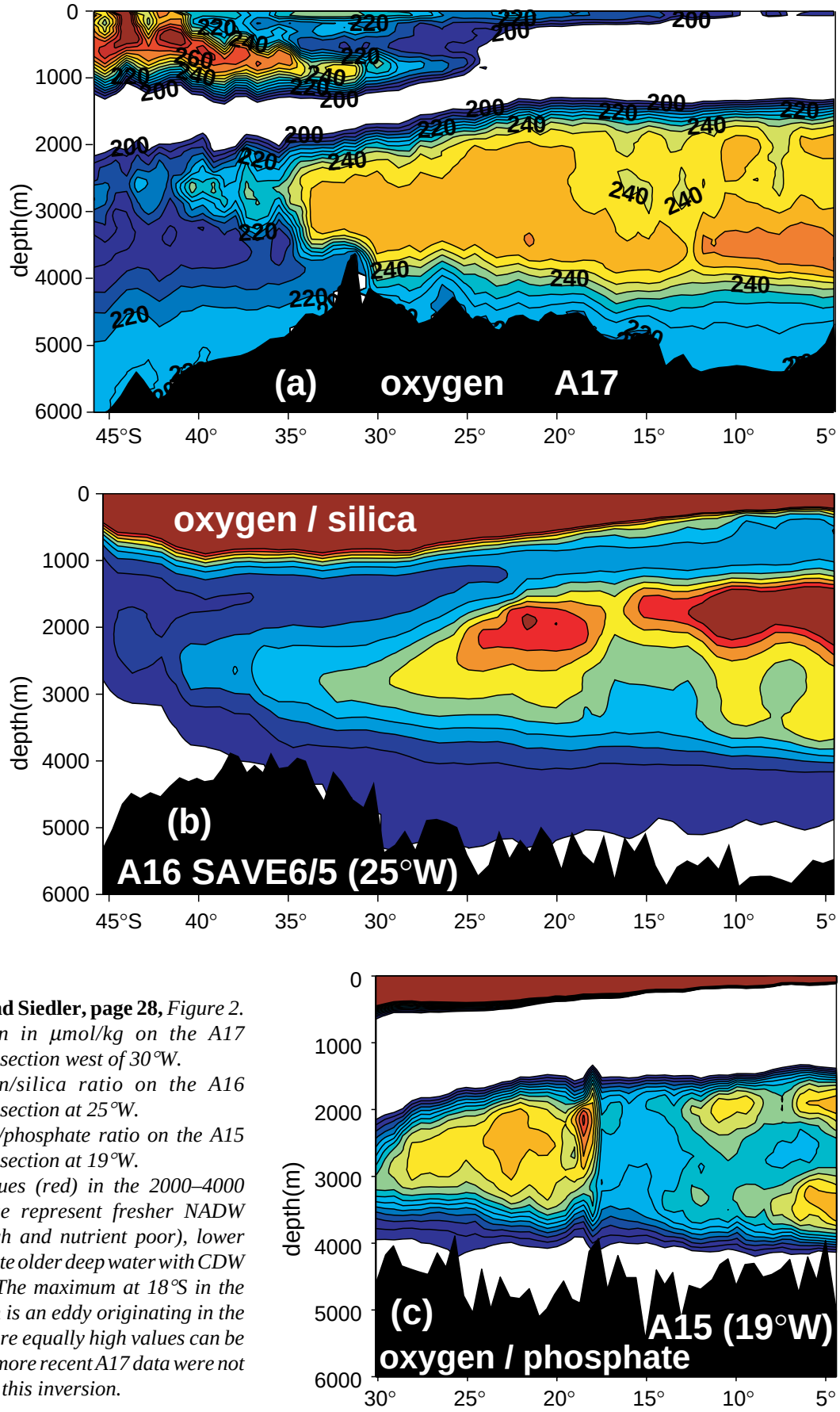

Vanicek and Siedler, page 28, *Figure 2.*
(a) Oxygen in µmol/kg on the A17 meridional section west of 30°W.
(b) Oxygen/silica ratio on the A16 meridional section at 25°W.
(c) Oxygen/phosphate ratio on the A15 meridional section at 19°W.
Higher values (red) in the 2000–4000 depth range represent fresher NADW (oxygen rich and nutrient poor), lower values denote older deep water with CDW signature. The maximum at 18°S in the A15 section is an eddy originating in the DWBC where equally high values can be found. The more recent A17 data were not included in this inversion.

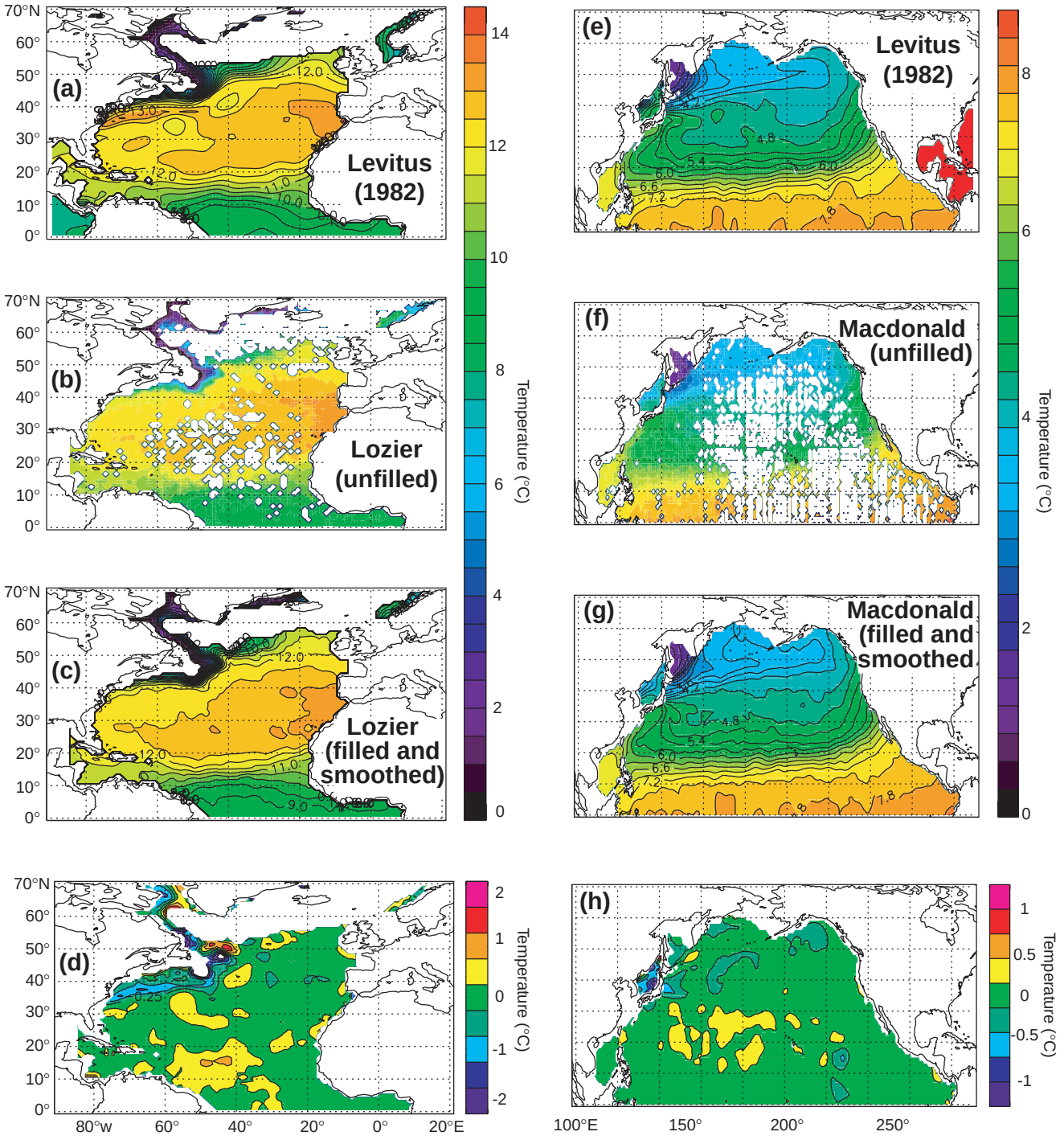

Grey et al., page 23, *Figure 3. Maps of temperature on the* $\sigma_0 = 27.0$ *potential density surface in the North Atlantic (a)–(d) and North Pacific (e)–(h). (d) and (h) show the difference between the new, smoothed climatologies and Levitus (1982). Contour intervals are 0.5°C for the N. Atlantic and 0.3°C for the N. Pacific.*

Climatological Hydrography of the North Atlantic

Stephen M. Grey and Keith Haines, Department of Meteorology, University of Edinburgh, UK; and Alison M. Macdonald, Woods Hole Oceanographic Institution, USA.
s.grey@ed.ac.uk

The most widely used climatological hydrography is Levitus (1982) and the updated versions Levitus (1994, 1998) (we have yet to access the 1998 atlas). These are very comprehensive data sets, set out on a $1\times1°$ global grid, describing the mean state of the ocean based on available CTD, XBT and bottle data. In order to produce a complete climatology, Levitus has had to heavily smooth the data. In some areas of the world ocean, such as the South Pacific, this is necessary due to the scarcity of data in these regions. However, such large-scale smoothing does wash out small-scale features and, especially when performed on depth surfaces, can distort water properties where isopycnals slope strongly.

Lozier et al. (1995) describe a climatology of the North Atlantic, presenting oceanic properties which are gridded and smoothed on potential density surfaces. A 1x1° gridded data set of temperature, salinity and oxygen content is obtainable from Woods Hole Oceanographic Institution* provided as hydrobase (Curry, 1996), but this provided data is unsmoothed and has holes in the grid where insufficient data were available. This does permit the user to choose their own smoothing algorithms but also makes the data less easy to access and use. We have filled in the holes and smoothed these data and reprojected back onto depth levels to produce a complete hydrography of the North Atlantic from the equator to 70°N and 85°W to 20°E in a similar format to Levitus (1982). This complete data set should be more useful for anyone initialising or running models or attempting other diagnostic calculations who do not wish to develop their own smoothing techniques. The filling and smoothing methods are described below.

All processing was performed on local potential density surfaces thus unrealistic mixing of water masses is avoided. Smoothing was kept to small scales to preserve resolution. There are no data in regions where the ocean is less than 200 m deep.

The grid of the hydrography is similar to Levitus. It has horizontal resolution of 1° and depth levels are the same to 1500 m. Below this depth, the depth levels become further apart in Levitus but stay at 100 m intervals in the original Lozier and the smoothed Lozier hydrographies.

The figures below show fields taken from the smoothed Lozier data set. For comparison, the equivalent fields from Levitus (1982) are also shown. In all cases, the Lozier hydrography is shown in the top frame.

*Obtainable by anonymous ftp from flotsam.whoi.edu under the directory pub/hydrobase.

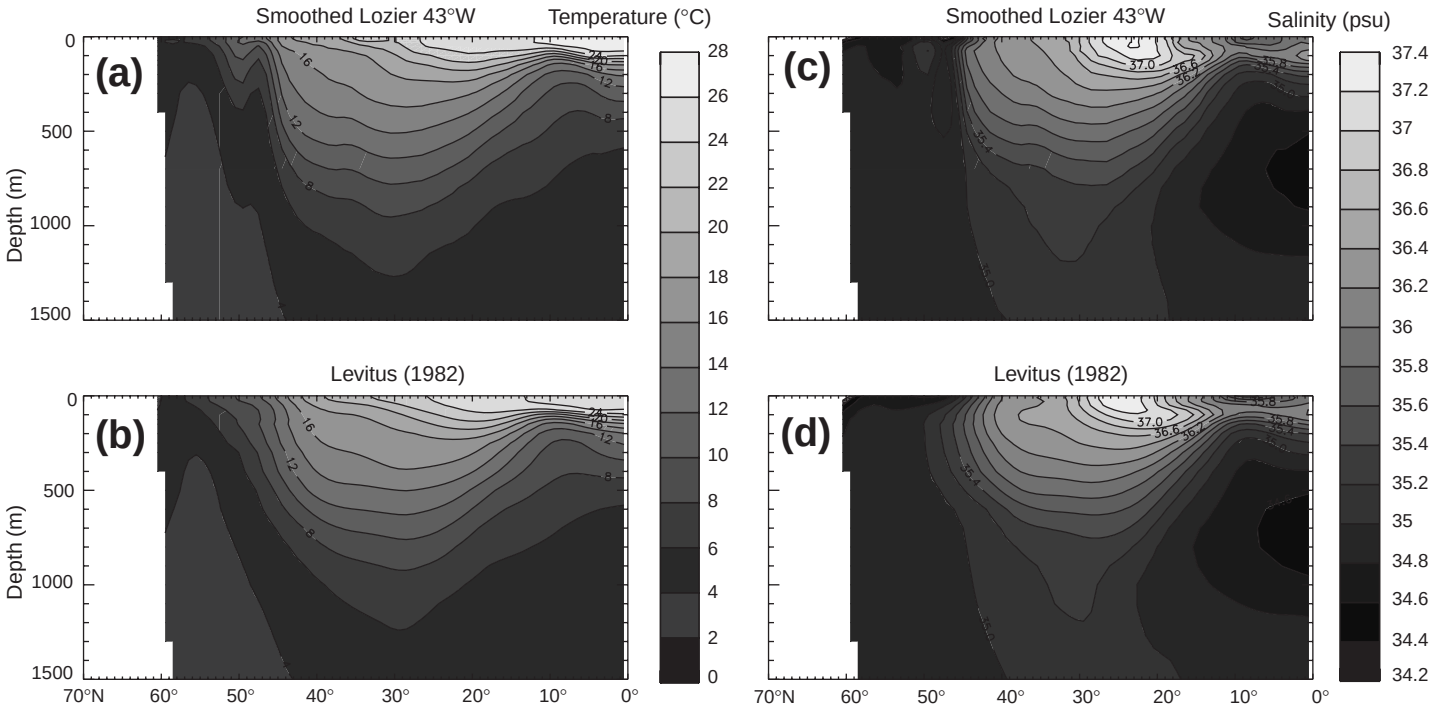

Figure 1. Cross-sections along longitude 43°W. (a) and (b) show temperature from the smoothed Lozier and Levitus (1982) data sets respectively. (c) and (d) show salinity from smoothed Lozier and Levitus (1982) respectively.

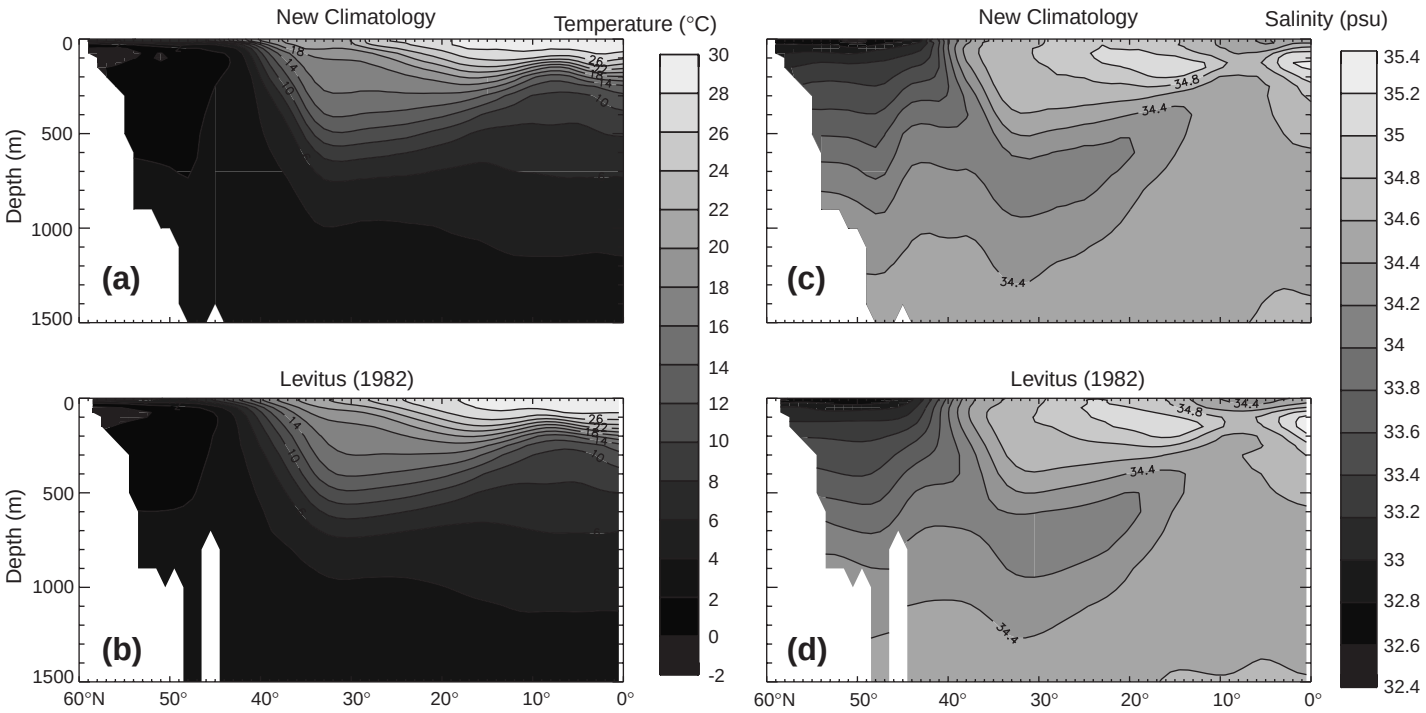

Figure 2. Cross-section along longitude 150°E in the Pacific Ocean. (a) and (c) are from the smoothed Macdonald climatology and (b) and (d) from Levitus (1982). (a) and (b) show temperature and (c) and (d) show salinity.

Fig. 1 shows north–south sections of temperature and salinity. This longitude crosses the Gulf Stream extension at approximately 45°N which can be clearly seen as a sharp front in the smoothed Lozier cross sections. The front is far broader in the Levitus hydrography due to the greater smoothing employed by Levitus.

Figs. 3a-d (page 22) show potential temperature on the $\sigma = 27.0$ surface in the N. Atlantic and demonstrate the degree of filling and smoothing compared to Levitus (1982), as well as the differences in the final analysed fields 3d. Fig. 3c can be compared to Lozier et al. (1995) Fig. 25. The improved spreading path of the Mediterranean water is clearly seen as well as the improved properties south of the Gulf Stream front.

Climatological hydrography of the North Pacific

Alison Macdonald and Toshio Suga have used the same techniques as Lozier et al. to produce a hydrography of the North Pacific**. Some results from this analysis can be found at http://www.oce.orst.edu/po/research/alm and in Macdonald et al. (1999). We have performed the same procedures used for the North Atlantic to fill and smooth these Pacific data giving complete fields from the equator to 62°N on a regular 1° grid on depth levels. The Pacific data has had the T/S smoothed twice where in the N. Atlantic only one smoothing pass was used. Fig. 2 shows meridional cross sections of temperature and salinity and Figs. 3e–h show the potential temperature, and differences thereof, on the 27.0 potential density surface.

**Obtainable by anonymous ftp from dingo.oce.orst.edu under the directory pub/hydrobase.

How to obtain the data sets

These data sets are available by anonymous ftp from mist.met.ed.ac.uk in directory pub/misc. For security reasons attempts to list this directory return nothing but the files can be down-loaded by typing

get n_atl.gz get n_pac.gz

The files needs to be unzipped and are in FORTRAN unformatted style. More information on reading the files, the grids and depth levels can be obtained from the same directory:

get n_atl.readme get n_pac.readme

Filling and smoothing

To produce the complete smoothed fields, the data grid was first filled, then T/S properties were smoothed on neutral surfaces once, then the depths of the surfaces alone were smoothed once more. This method always considers the density field local to the point being filled or smoothed.

Fig. 4 shows a grid-point on a depth level, z, (solid line), and the eight surrounding points, each point has a temperature and salinity. The grid-points are separated by 1° intervals. The first step of the process is to find the mean in situ density of the nine grid-points, σ, which will be used as the neutral density surface for smoothing and filling. Then, by linear interpolation vertically along the water columns, the position of this neutral surface (referenced to

the depth level, z) is determined. The neutral density surface, σ, is shown on the diagram as the dashed lines. It is from the interpolated property values on this surface that the filled or smoothed grid-point values are determined.

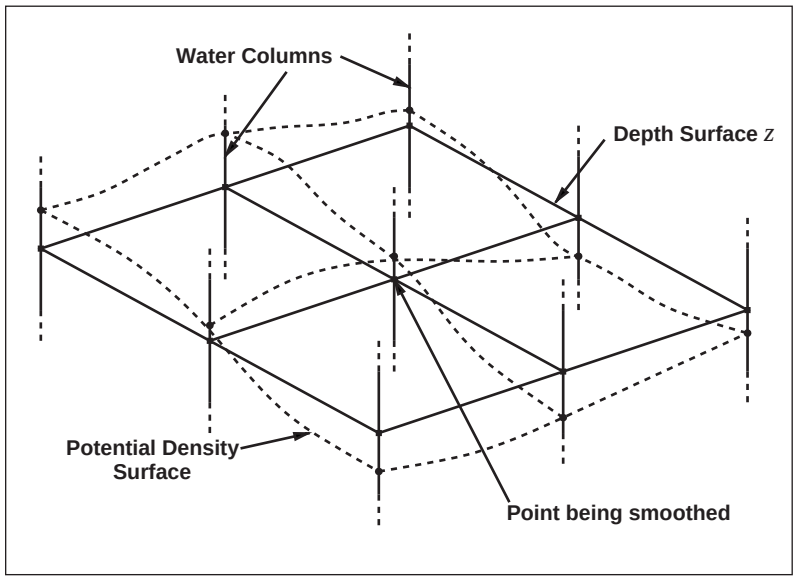

Figure 4. Illustration of the local neutral density smoothing method.

Filling

Only those points which have no data are filled, points with data already are left unchanged. Each missing point is given the mean temperature and salinity values on the neutral density surface, σ, of the surrounding points. Points are only filled if there are 5 or more surrounding data available. This process is iterated many times, hence holes in the grid are filled from the outside inward. When no more points can be filled with the minimum criterion of 5 surrounding data, then the limit is lowered to 4 for the next iteration. Further passes are then made with the criterion set at 5 again. Many repeats were required to fill the deeper levels.

Smoothing

There are two smoothing techniques which have been employed, the first smoothes temperature and salinity on density surfaces and the second smoothes just the depths of these surfaces.

In the first, the properties at the grid-point under consideration (the central point of the square in Fig. 4) are set to the mean of the T and S values on the neutral density surface, σ. This has the effect of smoothing the temperature, salinity and the depth of that surface.

The second method of smoothing finds the neutral density surface as before. However the new property values are determined from where the surface, σ, intersects the central water column only. This, in effect, smoothes the depth without changing T/S properties on the surfaces.

With this smoothing scheme, there are problems near the surface. If the neutral density surface, σ, outcrops in some of the nine water columns, a cold near surface bias would be introduced. To combat this, if outcropping occurs on more than four of the nine points examined, then the point is considered to be part of the mixed layer and it's properties are determined by averaging surface values of T and S over all nine grid points. With this modification, no overall decrease in SST is found after smoothing.

References

Curry, R. G., 1996: A database of hydrographic stations and tools for hydrological analysis. Tech Rep. WHOI-96-01, 44pp., Woods Hole Oceanographic Institution, USA.

Levitus, S., 1982: Climatological atlas of the world ocean. Professional Paper 12, NOAA, USA.

Levitus, S., 1994: World Ocean Atlas 1994 CD-ROM Sets. Informal Report 13, National Oceanographic Data Center, USA.

Lozier, M. S., W. B. Owens, and R. G. Curry, 1995: The climatology of the North Atlantic. Prog. Oceanogr., 36, 1–44.

Macdonald, A. M., T. Suga, and R. G. Curry, 1999: An isopycnally averaged North Pacific climatology. J. Geophys. Res., submitted.

The Origin of Waters Observed along 137°E

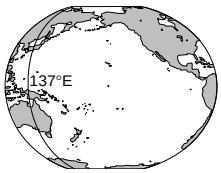

Frederick M. Bingham, University of North Carolina at Wilmington, USA;
Toshio Suga and Kimio Hanawa, Tohoku University, Japan. binghamf@uncwil.edu

Time series hydrographic observations in the ocean are valuable pieces of information in assessing interannual and interdecadal variability. An important and interesting time series is the set of observations taken along 137°E in the western Pacific (Fig. 1). Other long-term ocean time series have focused on measurements at a single station like the Hawaii Ocean Time series or the Bermuda Atlantic Time Series programmes or Ocean Weather Station P, or on shallow, upper ocean expendable temperature and salinity measurements that cross ocean basins. In contrast, the 137°E section cuts across the entire western Pacific, measuring shallow, intermediate and deep waters from tropical and subtropical regions.

The 137°E measurement programme is operated by the Japan Meteorological Agency (JMA). Since it began, it has been used for pollution monitoring and studies of climate and El Niño. Whatever the purpose of the measurements, the sampling scheme has remained nearly the same for 30 years, constituting a unique record of long-term variability in the gyre-scale structure of the western North Pacific. With few exceptions, two hydrographic sections are made each year, one in winter and one in summer, along 137°E from Japan to the coast of New Guinea (since 1988 only as far south as 2°N).

There has been a recent interest in water mass variability along 137°E and its relationship to climate changes in the North Pacific (Kato, 1998). The variability can only be understood in terms of the origins and flow paths of the water masses themselves.

The physical processes which form the water masses observed along 137°E are many and varied. We can see waters formed by standard mid-latitude subduction (e.g. North Pacific Tropical Water; NPTW), strong buoyancy forcing south of the Kuroshio front (Subtropical Mode Water; STMW) and lateral and/or vertical mixing in the mixed-water region between the Kuroshio and Oyashio (North Pacific Intermediate Water; NPIW). We also see waters that are insulated from the surface and do not have a formation process as such (North Pacific Tropical Intermediate Water; NPTIW) and waters have travelled very far from their point of formation (e.g. Antarctic Intermediate Water; AAIW).

Using annual average data from the National Oceanographic Data Center's World Ocean Atlas 1994 (WOA), maps of acceleration potential or Montgomery streamfunction relative to 2000 m were prepared for a number of isopycnals between 23.0 and 27.2σ_θ.

One example of such a map (Fig. 1) indicates the placement of the 137°E section within the context of the tropical and subtropical Western Pacific. It cuts through the recirculation zone of the subtropical gyre, the dynamic trough between the North Equatorial Current and North Equatorial Countercurrent and the tropical current systems near the equator. On the basis of maps such as this one, the authors' intuition and knowledge and many previous studies, we present a schematic picture of the types of water masses observed along 137°E, juxtaposed with salinity measured on one realisation of the 137°E section (Fig. 2).

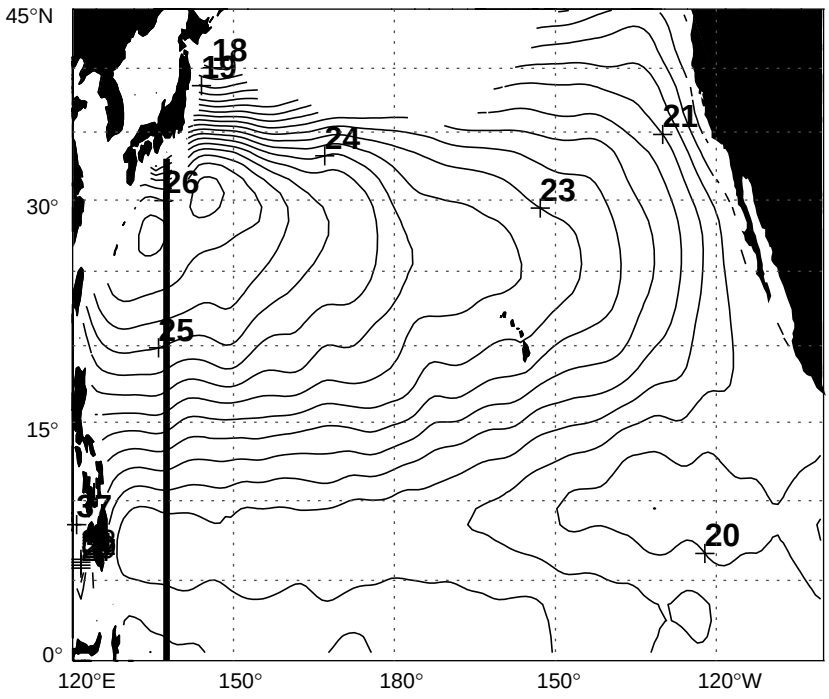

Figure 1. Acceleration potential ($m^2\ s^{-2}$) relative to 2000 m on 25.0σ_θ surface from the WOA. Location of the 137°E section is indicated by a heavy line.

Directly ventilated waters are ones where a direct flow path exists between the water's outcrop region and 137°E. These waters are mainly comprised of the high salinity NPTW. STMW is also directly ventilated, but its formation process is enhanced by strong lateral induction at its formation region (Qiu and Huang, 1995). Recirculating waters are those which do not outcrop in the subtropical gyre, but recirculate at the base of the gyre. NPIW is the principal example of this. Its vertical salinity minimum can be seen in the salinity section north of 20°N. Note that not all salinity minimum water recirculates within the subtropical gyre. The southern limit of the subtropical gyre

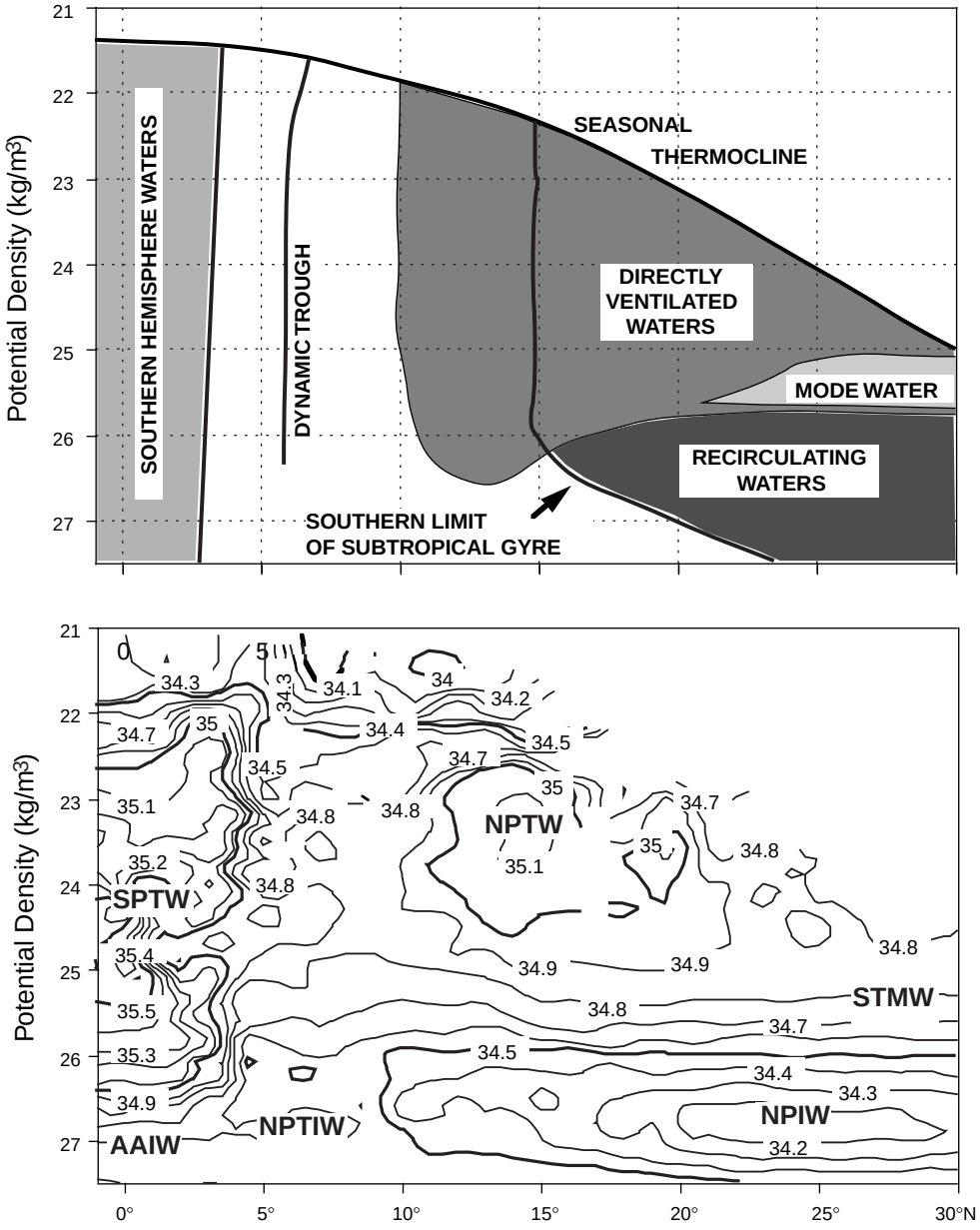

Figure 2. Top panel: Schematic distribution of waters along 137°E according to original formation processes. Bottom panel: Salinity (pss) along 137°E measured during January 1986. Contour interval is 0.1. The names and locations of some of the important water masses are superimposed.

marks the southernmost latitude where waters, having passed through 137°E, turn right at the western boundary and participate in the Kuroshio return flow. South of the southern limit, waters turn left at the boundary and flow towards the tropical Pacific. Some of the directly ventilated waters, particularly those that have outcropped in the north-eastern part of the gyre do not circulate in the subtropical gyre, but cross into the tropical circulation. At the southern end of the 137°E section, there is a sharp water mass boundary between 3 and 4°N, sloping equatorward with depth. At the northern side of this boundary lies the North Equatorial Countercurrent and Northern Subsurface Countercurrent. South of this boundary, one finds waters whose origins can be traced to the southern hemisphere, principally South Pacific Tropical Water (SPTW) and AAIW. Between about 10°N and 3–4°N, there is a set of upper and intermediate waters whose origins and dynamics have been little studied.

Given that the waters observed along 137°E have such diverse origins, we expect the characteristics of variability in each of these waters to be different. Using variability observed in a time series such as the 137°E line to infer changes in formation processes is problematic. We have evidence (not presented here) that along-path mixing is an important, perhaps primary, factor in determining what is observed at 137°E. Much of this mixing takes place between waters of different ages formed in different regions, where the physical processes involved in formation are completely different. Deconvolving this variability in the presence of unknown vertical and horizontal diffusivities will be a major challenge during the synthesis phase of WOCE.

Acknowledgements

Research funded by the National Science Foundation under grant #OCE-9711300, and the Japan Society for the Promotion of Science under its Short-term Invitation Fellowship program.

References

Kato, A., 1998: Decadal scale variations of surface and intermediate water masses in the subtropical and tropical western North Pacific. Masters Thesis, Tohoku University, Graduate School of Science (in Japanese).

Qiu, B., and R. Huang, 1995: Ventilation of the North Atlantic and North Pacific: Subduction versus obduction. J. Phys. Oceanogr., 25, 2374–2390.

Zonal Fluxes in the Deep Layers of the South Atlantic

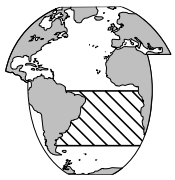

M. Vanicek, Woods Hole Oceanographic Institution, USA., and G. Siedler, Institut für Meereskunde, Kiel, Germany. mvanicek@whoi.edu

The South Atlantic serves as the passage between the key water mass formation regions of the global ocean. Cold North Atlantic Deep Water (NADW), having been formed by convection and mixing in the northern North Atlantic, flows southward at depth, and the compensating return flow at intermediate and shallow levels transports warmer water from the Pacific and Indian Oceans to the North Atlantic. Also cold subpolar and polar water masses, having been formed mostly in the Weddell Sea, and the Circumpolar Deep Water (CDW), arrive from the south at abyssal layers and contribute to the global overturning cell.

The circulation of the NADW within the western South Atlantic, described previously in the literature extends from large-scale patterns (Wüst, 1935; Defant, 1941; Reid, 1989) to very complex ones with several recirculation cells (Durrieu de Madron and Weatherly, 1994; Larque et al., 1997). The distribution of oxygen given by Wüst (1935) indicated three tongues with oxygen-rich water with NADW-characteristics: along the South American continental slope, eastward close to the equator and off the South American coast over the seamount chain near 20°S, the Vitoria–Trinidade Ridge. After Wüst's "spreading" hypothesis the water spreads down the property gradient. The particularly interesting zonal branching of the NADW near 20°S has been suggested also in various circulation schemes that were assembled from modern hydrographic data (Reid, 1989; Durrieu de Madron and Weatherly, 1994; Friedrichs et al., 1994; Larque et al., 1997; Zangenberg and Siedler, 1998). But in most of them the flow does not cross the Mid-Atlantic Ridge (MAR) and recirculates to the north within the Brazil Basin. The recent results obtained from direct float observations in the depths of NADW (Hogg and Owens, 1998) show that away from the western boundary the zonal flows dominate over the meridional flows. Some of the floats seem to cross the MAR between 20°S and 25°S.

Data set preparation and analysis methods

The deep zonal fluxes, emphasised herein, are determined from hydrographic, nutrient and tracer data using a linear box-inverse model (Wunsch, 1978). Altogether 19 high-

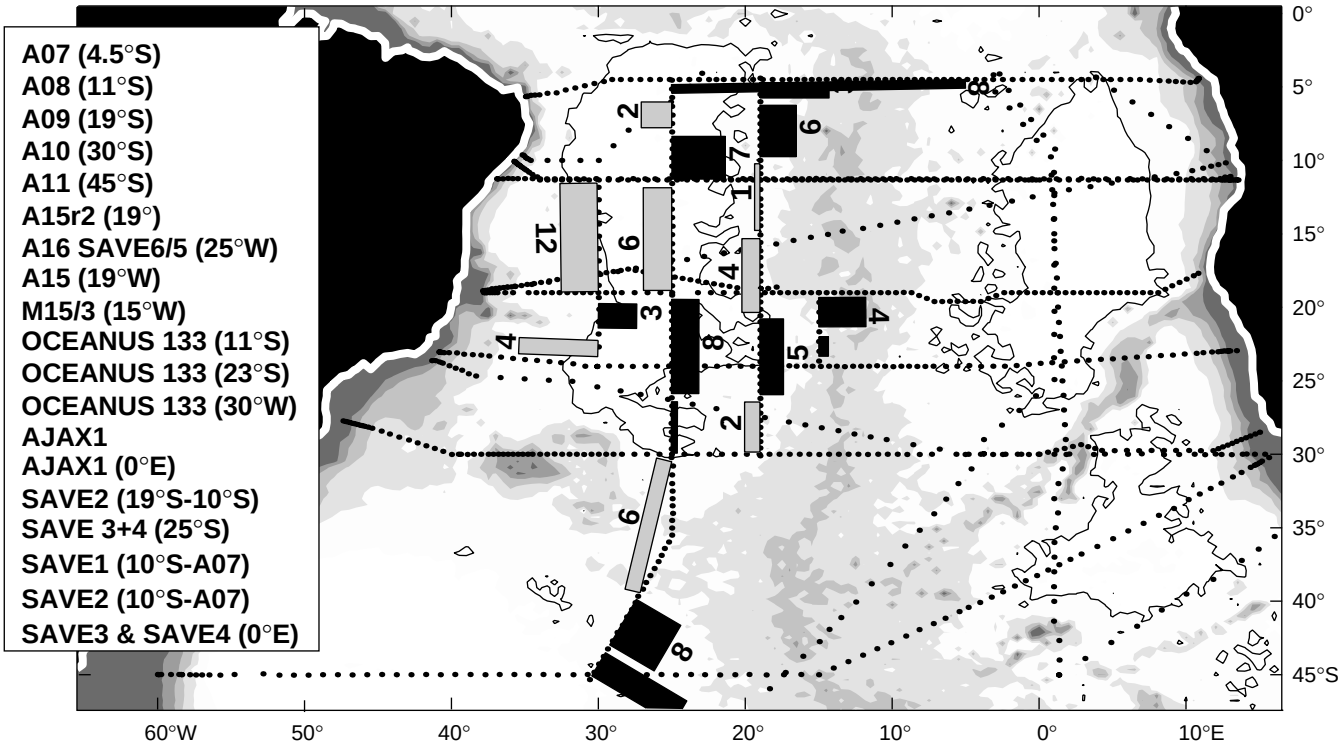

Figure 1. Zonal transport [Tg/s] in the whole NADW layer, divided into separate bands which dominate the spreading directions for the meridional sections in Oceanus 133 at 30°W, A16 at 25°W , A15 at 19°W and A9 (meridional part) at 15°W. Eastward transports are black, westward ones are grey. Transports values are rounded to whole numbers and printed on the side of the bar which is in the direction of flow. The layer is defined by neutral density surfaces γ_n: 27.88–28.12. The used hydrographic sections are listed on the left margin and the corresponding locations are represented as dots in the figure.

quality sections, mostly measured during the World Ocean Circulation Experiment (WOCE), were used (Fig. 1). Some pre-WOCE sections were necessary to fill in for the non-available meridional WOCE sections.

Some parameter values were missing on certain stations or sections. In order to obtain a complete data set at each station a multiple linear regression (MLR after Holfort et al., 1998) was applied. This interpolation method, which makes use of the correlation between different parameters, enabled us to infer missing values and to include the nutrient and tracer measurements in the inverse model with the spatial resolution of the corresponding CTD data.

Table 1. List of the used conservation equations. In the second column is the vertical range (net: integrated top-to-bottom, layers: below the euphotic zone) for which the conservation is prescribed.*

	vertical range	horizontal range	prescribed value
southward meridional salt flux	net	zonal sections	-26.7 10^6 kg/s
salt conservation	all layers	all Boxes	0
southward meridional phosphate flux	net	zonal sections	-4 kmol/s
silica conservation	layers*	all Boxes	0
Brazil Current (10° S-A10)	0-600 dbar	west 43.5° W	-10 Sv
Benguela Current (10° S-A10)	0-1000 dbar	east WVR	14 Sv
AABW (10° S-A10)	AABW	west MAR	7 Sv
AABW (10° S-A10)	AABW	Vema Channel	4 Sv
AABW (4.5° S-A7)	θ <1.9° C	west MAR	3.1 Sv
LNADW/AABW	γ_n >28.11	Angola-Cap B.	0 Sv
A11 after Saunders and King, 1995	various constraints		

The main assumptions are that the ocean is in steady state and that the flow occurs in layers between neutral density surfaces (Jackett and McDougall, 1997). To determine the vertical boundaries for these layers a detailed water mass analysis was performed, incorporating the tracer information from the whole South Atlantic. As a result the water column was divided into 11 layers. The information about water mass interfaces was also used for the choice of initial reference levels (LNM) for the calculation of the a-priori geostrophic velocity field.

Constraints for the inverse model (Table 1) are an integral meridional salt and phosphate transport, as well as the overall salt and silica conservation, resulting in one equation per layer and property (for silica below the euphotic zone) in each box.

Additional constraints for the mass transport inferred from direct current observations (lower part of Table 1) are: southward Brazil Current transport of 10 Sv after Holfort and Siedler (1998), mean northward transport of the Benguela Current of 14 Sv between Walvis Ridge (WVR) and Africa (Garzoli et al., 1997), the inflow of 7 Sv of Antarctic Bottom Water (AABW) to the Brazil Basin (Hogg et al., 1999), the northward flow of AABW out of Brazil Basin of 3.1 Sv corresponding to the sum of the direct measurements further north, in the equatorial passage at ca. 35°W (Hall et al., 1997; Rhein et al., 1998) and in the Romanche and Chain Fracture Zones (Mercier and Morin, 1997).

Zonal transports

All these constraints were used to set up a system of linear equations for the unknown barotropic velocity component. After the inversion which minimises the deviation from an initial state using the Singular Value Decomposition technique (SVD), an estimate of the absolute geostrophic velocity profile for each station pair was obtained.

The resulting zonal mass transport was divided into separate bands (Fig. 1) according to changes in flow direction or to changes in the strength of the corresponding cumulative transport (not shown). A clear meridional separation in the direction of the zonal transport in the NADW layers can be observed. It shows an eastward flux in the Brazil Basin between 20–25°S. This flow begins near the Vitoria–Trinidade Ridge and continues to the Rio de Janeiro Fracture Zone of the MAR. To the north of this eastward motion deep water returns to the west between 10–15°S. An additional band with eastward flow direction occurs just north of 10°S. These features from the inverse model are in qualitative agreement with the currents directly measured by deep floats (Hogg and Owens, 1998).

The eastward flow between 20°S and 25°S consists of relatively fresh NADW. It is characterised by its maximum in oxygen and salinity and low concentrations in silica, phosphate and terrigenic helium compared with the high nutrient and δ^3He values of the CDW. Due to the contrasting property concentrations of the NADW and CDW the younger NADW coming from the Deep Western Boundary Current (DWBC) possesses higher values, for example, of the ratio of oxygen/nutrient. Although the exact values of this ratio are not important, the location of minima and maxima on the 25°W section shows clearly the NADW coming from the western boundary (high values – red in Fig. 2b, page 21) at about 22°S and the older deep water (lower values) in the westerly flow between 20 and 10°S. At the same latitude band the older NADW can be found in

the low-oxygen concentrations of the A17 section at 31°W (Fig. 2a) and in low values of the oxygen/phosphate ratio in the A15 section at 19W (Fig. 2c). The latter shows also a core of newer NADW at 10°S and second large core between 20–25°S, which corresponds to the eastward flow obtained from the inverse model. This eastward flow of fresher NADW can be seen even at 15°W, just west of the MAR as a low value of the product terrigenic helium times phosphate, which reaches down to 3500 m (not shown).

A similar pattern can be seen in the meridional distribution of oxygen on several density surfaces within the NADW for the 25°W (A16) section (Talley and Johnson, 1994) and also in the corresponding zonal mean flow from current meter and RAFOS float data (Hogg, 1999).

The broad band of easterly NADW flow between 20°S and 25°S obtained from the inverse model appears to originate in the DWBC along the western boundary and could well supply the "Namib Col Current" (Speer et al., 1995). This is also the band of latitudes at which the minimum depth of the MAR is the deepest (Fig. 3) and where the Rio de Janeiro Fracture Zone is located at 22°30'S and 13°15'W with a depth of 3900 m and a width of 35 km. It could be the place where approximately 4 Sv of NADW cross the MAR to the Angola Basin.

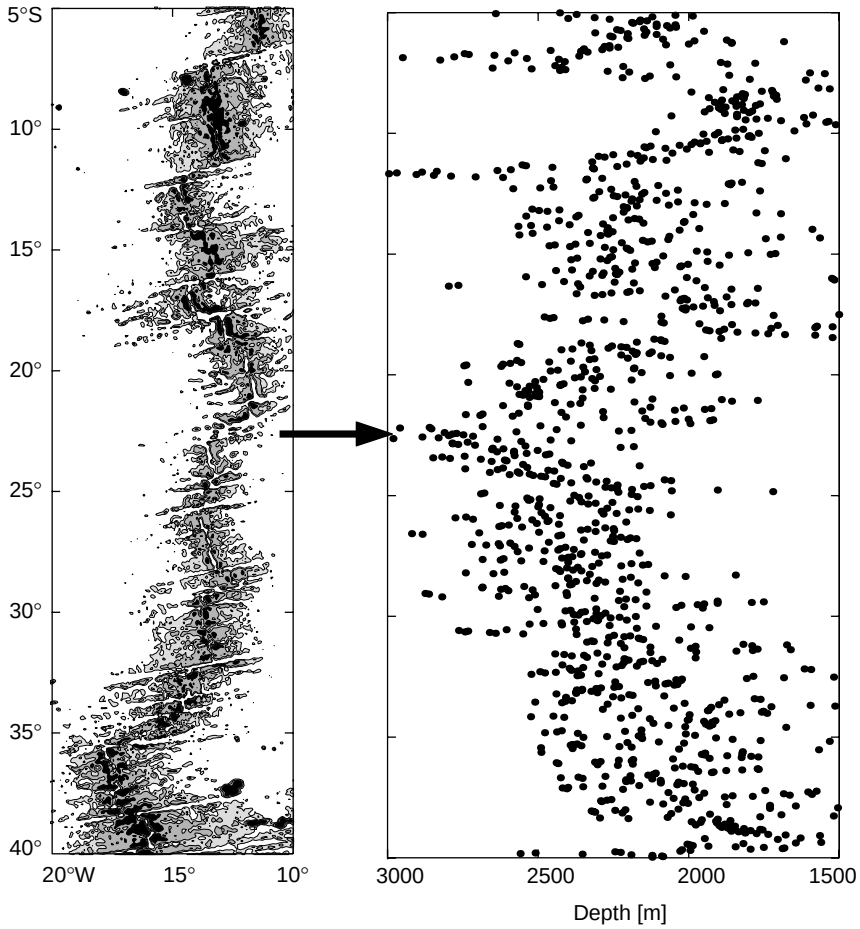

Figure 3. Left: topography of the Mid-Atlantic Ridge from the TOPEX data set (Smith and Sandwell, 1997); black: depth <2500 m, white: depth >3300 m, grey: 2500–3300 m, divided at 3000 m. Right: the depths of the shallowest point of each about 5 longitudinal degrees wide zonal strip of the fully (2') resolved TOPEX topography along the MAR. The arrow represents the latitude of the Rio de Janeiro Fracture Zone.

Acknowledgements

This study is a WOCE contribution. The assistance of the staff of the Department of Marine Physics of the Institut für Meereskunde at Kiel University in the observations and the data processing was much appreciated. We are also grateful to all the oceanographers, PIs and scientists who collected and let us use the data, either directly or by making them publicly available. Thanks go to N. Hogg and others from the Department of Physical Oceanography at the Woods Hole Oceanographic Institution for current support and useful discussions, and to M. Arhan for providing the more recent A17 data.

References

Defant, A., 1941: Quantitative untersuchungen zur statik und dynamik des Atlantischen Ozeans. Wiss. Ergebnisse dtsch. Atlant. Exped. "Meteor", 6(2), 191–260.

Durrieu de Madron, X. , and G. Weatherly, 1994: Circulation, transport and bottom boundary layers of deep currents in the Brazil Basin. J. Mar. Res., 52, 583–638.

Friedrichs, M. A. M., M. S. McCartney, and M. M. Hall, 1994: Hemispheric asymmetry of deep water transport modes in the western Atlantic. J. Geophys. Res., 99 (C12), 25165–25179.

Garzoli, Silvia L., G. J. Goni, A. J. Mariano, and D. B. Olson, 1997: Monitoring the upper south-eastern Atlantic transports using altimeter data. J. Mar. Res., 55 (3), 453–481.

Hall, M. M., M. S. McCartney, and J. A. Whitehead, 1997: Antarctic bottom water flux in the equatorial western Atlantic. J. Phys. Oceanogr., 27, 1903–1926.

Hogg, N. G., 1999: Deep circulation. pages Chapter 4.6, submitted. International Geophysics Series, Academic Press.

Hogg, N. G., and W. B. Owens, 1999: Direct measurement of the deep circulation within the Brazil Basin. Deep-Sea Res., 46(II), 335–353.

Hogg, N. G., G. Siedler, and W. Zenk, 1999: Circulation and variability at the southern boundary of the Brazil Basin. J. Phys. Oceanogr., 29, 145–157.

Holfort, J., K. M. Johnson, B. Schneider, G. Siedler, and D. W. R. Wallace, 1998: Meridional transports of dissolved inorganic carbon in the South Atlantic Ocean. GBC, 12(3), 479–499.

Holfort, J., and G. Siedler, 1998: The oceanic transports of heat and nutrients in the South Atlantic. J. Phys. Oceanogr., submitted.

Jackett, D., and T. McDougall, 1997: A neutral density variable for the world's oceans. J. Phys. Oceanogr., 27(2), 237–263.

Larque, L., K. Maamaatuaiahutapu, and V. Garcon, 1997: On the intermediate and deep water flows in the South Atlantic Ocean. J. Geophys. Res., 102(C6), 12425–12440.
Mercier, H., and P. Morin, 1997: Hydrography of the Romanche and Chain Fracture Zone. J. Geophys. Res., 102, 10373–10389.
Reid, J. L., 1989: On the total geostrophic circulation of the South Atlantic Ocean: Flow patterns, tracers and transports. Prog. Oceanogr., 23, 149–244.
Rhein, M., L. Stramma, and G. Krahmann, 1998: The spreading of Antarctic Bottom Water in the tropical Atlantic. Deep-Sea Res., 45, 507–527.
Saunders, P.M., and B. A. King, 1995: Oceanic fluxes on the WOCE A11 section. J. Phys. Oceanogr., 25(9), 1942–1958.
Smith, W. H. F., and D. T. Sandwell, 1997: Global seafloor topography from satellite altimetry and ship depth soundings. Science, 277, 1956–1962.
Speer, K. G., G. Siedler, and L. D. Talley, 1995: The Namib Col Current. Deep-Sea Res., 42(11/12), 1933–1950.
Talley, L. D., and C. Johnson, 1994: Deep, zonal subequatorial currents. Science, 263, 1125–1128.
Wunsch, C., 1978.: The North Atlantic general circulation west of 5°W determined by inverse methods. Rev. Geophys. Space Phys., 16(4), 583–620.
Wüst, G., 1935: Schichtung und zirkulation des Atlantischen Ozeans. das bodenwasser und die stratosphaere. Wiss. Ergebn. Dt. Atl. Exp. “Meteor” 1925–1927, 6, 1–288, Berlin.
Zangenberg, N., and G. Siedler, 1998: The path of the North Atlantic Deep Water in the Brazil Basin. J. Geophys. Res., 103, 5419–5428.

Indian Ocean Workshop Promotes Co-operation

Piers Chapman, US WOCE Office Director

The University of Miami, with assistance from the US WOCE Office, hosted a workshop 10–11 May 1999 to encourage cooperation between Principal Investigators (PIs) interested in the variability of the northern Indian Ocean. The workshop, chaired by Fritz Schott, resulted from a recommendation made at the WOCE Indian Ocean workshop in New Orleans in September 1998. The Miami meeting brought together researchers from the US, Germany and India to discuss some of the latest results from the region. It is anticipated that their discussions will lead to collaborative work to synthesise the various data sets collected during the 1990s, including those collected with support from the Joint Global Ocean Flux Study and the Office of Naval Research, and thus expand our knowledge of, for example, water movement, heat and freshwater fluxes, and water mass variability.

Following a series of short talks on model results, attendees heard about the latest analyses of data from the Arabian Sea and Bay of Bengal. They then discussed aspects of the variability imposed by the alternating south-west and north-east monsoons. The main aim, however, was to talk about future collaborative work. To this end, the following topics were identified as being of particular importance (no relative ranking is implied by their order on this list):

1. Circulation and water mass pathways across the Arabian Sea.
2. Exchange across 8°N and basin-scale budgets for the basins to the north.
3. The response of the north-west Indian Ocean to the monsoons.
4. Circulation and water mass pathways of the Bay of Bengal.
5. Mechanisms of leakage around Sri Lanka.
6. Equatorial structure and variability (seasonal, inter-annual, and any linkages to the El Niño Southern Oscillation).

Obviously these topics are not mutually exclusive, and the same data sets and model studies (and PIs) will likely be involved in several. While attendees held initial discussions on how best to proceed, it was recognised that several PIs having known interests in the region were unable to attend. Therefore, it was left to follow-up correspondence to identify co-ordinators and group compositions for these topics. Schott (fschott@ifm.uni-kiel.de) will continue to coordinate activities and should be approached by other interested parties.

Schott also has been promoting a collection of WOCE papers on the Indian Ocean to be produced either as a dedicated volume in a specific journal or as a collection of papers at a later date. At the meeting, a list of over 40 papers in press or in preparation was checked and new additions were sought. The meeting attendees adopted 1 May 2000 as the deadline to submit papers for consideration in such a volume; journal and format will be announced later.

Circulation of the Southwest Pacific: WOCE section P11, Papua New Guinea to Tasmania

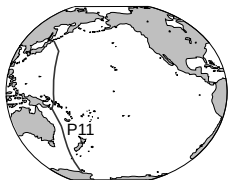

Serguei Sokolov and Stephen Rintoul, CSIRO Marine Research and Antarctic Cooperative Research Centre, Hobart, Australia

A roughly meridional section along 155°E from the Subtropical Front (approximately 45°S) to the Louisiade Archipelago at 12°S was occupied as part of the WOCE one-time survey (section P11S, Fig. 1, page 20). P11S is the first synoptic, full-depth meridional section through the deepest parts of the Tasman and Coral Seas. The section is used here to describe the water masses of the south-west Pacific and to quantify the top-to-bottom circulation of the Coral and Tasman Seas, with a particular focus on the zonal flows into and out of the western boundary of the South Pacific (Sokolov and Rintoul, 1999).

The primary circulation features of the region are shown schematically in Fig. 1. The primary inflow to the Tasman and Coral Seas is supplied by the South Equatorial Current (SEC), which crosses the P11 section as a wide band of west-flowing currents between 14 and 18°S. The SEC bifurcates at 18°S with the southern branch feeding the East Australian Current (EAC), and the northern branch re-circulating in the Gulf of Papua New Guinea. Along the southern coast of PNG the northern branch forms the New Guinea Coastal Undercurrent (NGCUC), which flows around the Louisiade Archipelago and enters the Solomon Sea. The EAC flowing south along the Australian coast separates from the coast at 30°S and can be traced as a continuous meandering eastward jet known as the Tasman Front. The circulation in the southern part of the Tasman Sea is dominated by transient eddies and standing gyres. An anticyclonic circulation cell located south of Tasmania appears to facilitate the exchange of water between the Tasman Sea and the Southern Ocean.

The two major inflows into the region, supplied by the SEC and the anticyclonic re-circulation in the southern part of the Tasman Sea, are clearly reflected in water properties distributions (Figs. 2a, b). The deep and bottom waters of the Tasman Sea are supplied directly from the south, while in the Coral Sea the major inflow in the layer below 2500 m depth occurs in the SEC. Two distinct areas of low salinity at the

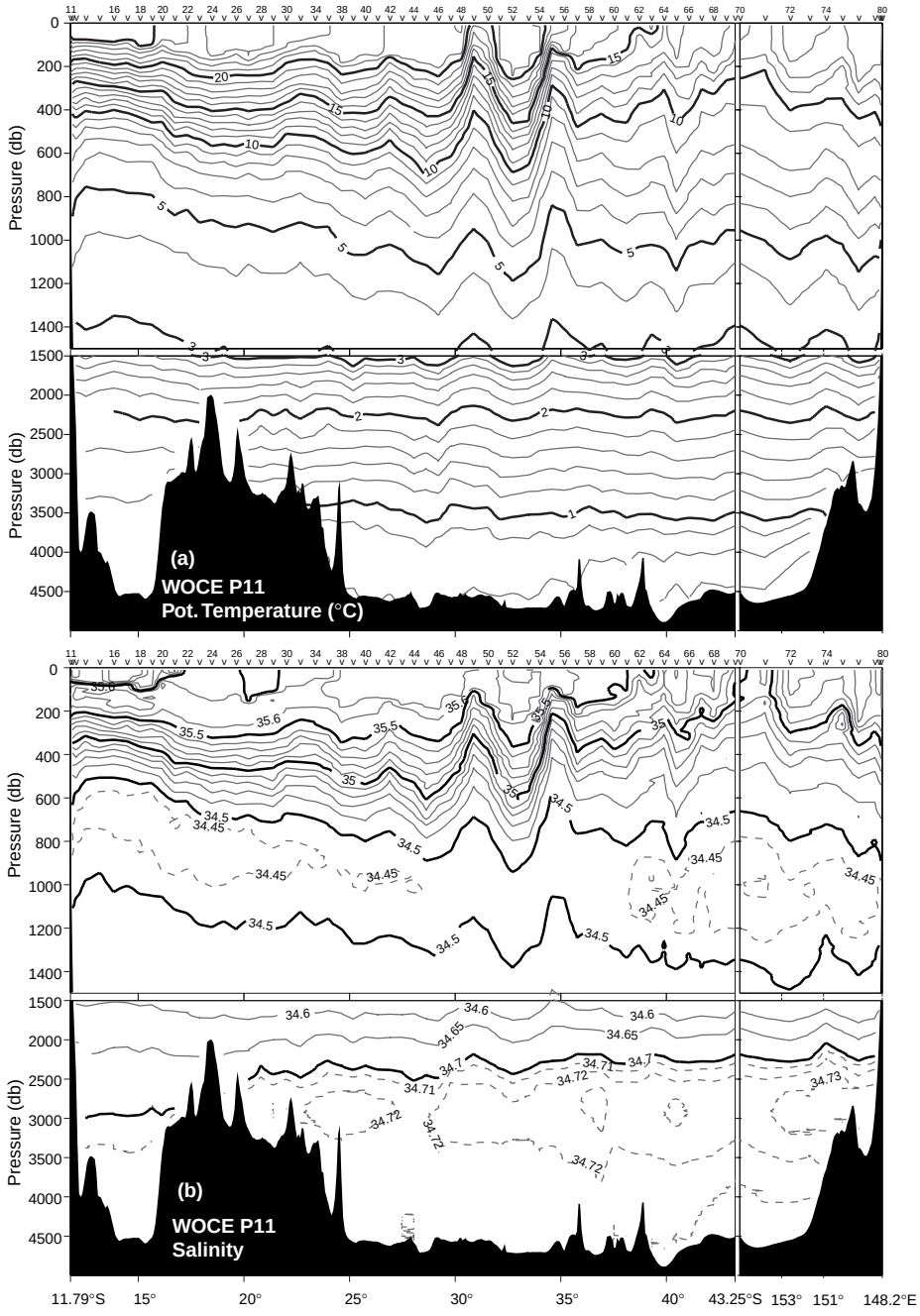

Figure 2. Potential temperature (°C) (a) and salinity (b) distributions along WOCE section P11.

depths of 800–1000 m mark the inflow of two varieties of Antarctic Intermediate Water (AAIW): one carried in the SEC by subtropical gyre circulation at the northern end of P11, and another by the anticyclonic re-circulation in the southern part of the Tasman Sea at the southern end of P11 (Fig. 2b). The Subantarctic Mode Water (SAMW), which forms lower thermocline waters, mirrors that of the AAIW below. The upper layers of the subtropical zone characterised by the shallow salinity maximum are occupied by the Subtropical Lower Water (SLW) which extends southward on P11 as far as the Subtropical Front at 38°S.

WOCE section P11 was carried out on RV Franklin in June–July 1993. A total of 80 stations were occupied. On each station a rosette sampler equipped with a CTD was lowered to within 10 m of the sea floor. Stations were spaced generally at intervals of 66 km, but at closer intervals (about 10-15 km) near the Tasmania and Papua New Guinea coasts. Continuous profiles of temperature, salinity and oxygen were obtained at each station, and water samples at 24 depths were analysed for salinity, oxygen and nutrients (Figs. 2a,b). Continuous underway measurements of velocity were obtained with a 150 kHz acoustic Doppler current profiler (ADCP).

The circulation: choice of reference level

Most studies of the circulation of the Coral and Tasman Seas have assumed a level of no motion at mid-depth. The most common choice, 1300 dbar, has been motivated more by the lack of measurements deeper than this rather than by evidence that the flow at this depth is weak. However, the few direct velocity measurements that exist suggest that, at least for the EAC and eddies spawned from the EAC, the currents extend very deep in the water column in this region (Boland and Hamon, 1970; Hamon, 1970; Mulhearn et al., 1988). These studies suggest that a reference level at mid-depth may underestimate the transport of the EAC by a factor of 1.6 or more, and that a near-bottom reference level is appropriate in the EAC.

Integrating the geostrophic velocity relative to the deepest common depth along the nearly-enclosed box defined by P11 results in a net inflow to the region of 3.6 Sv (Fig. 3). Noting that the sum of the absolute value of the station pair transports across the boundaries of the box is more than 500 Sv, the estimated imbalance is small. Including the Ekman transport for July, which is directed into the region across all boundaries, the resulting imbalance is about 8.7 Sv. The integrated geostrophic transport across the section relative to 2000 and 1300 db does not conserve mass. An attempt to use currents measured by the ADCP to reference the geostrophic velocities was rejected because the implied barotropic component is large and varies along the section in a way that shows little relation to the water mass distribution (no GPS heading information was available on this cruise). Transport relative to the deepest common depth is presented as our best estimate of the circulation, with no adjustment made to remove the remaining small imbalance.

The Coral Sea inflow

The primary inflow to the Tasman/Coral Sea is supplied by the SEC, which crosses the P11 section as a wide band of westward flow between 14 and 18°S with a total geostrophic transport of 55.4 Sv relative to the bottom. The SEC consists of three cores. The northern core carries 14 Sv of low oxygen thermocline and intermediate water as part of a tropical gyre, consisting of eastward flow along the equator in the Equatorial Undercurrent (EUC), southward flow in the central Pacific, westward flow in the northern branch of the SEC, and closed by equatorward flow in the low latitude western boundary current formed by the Great Barrier Reef Undercurrent (GBRUC)/NGCUC. The middle and southern cores of the SEC carry high oxygen water as part of the subtropical gyre.

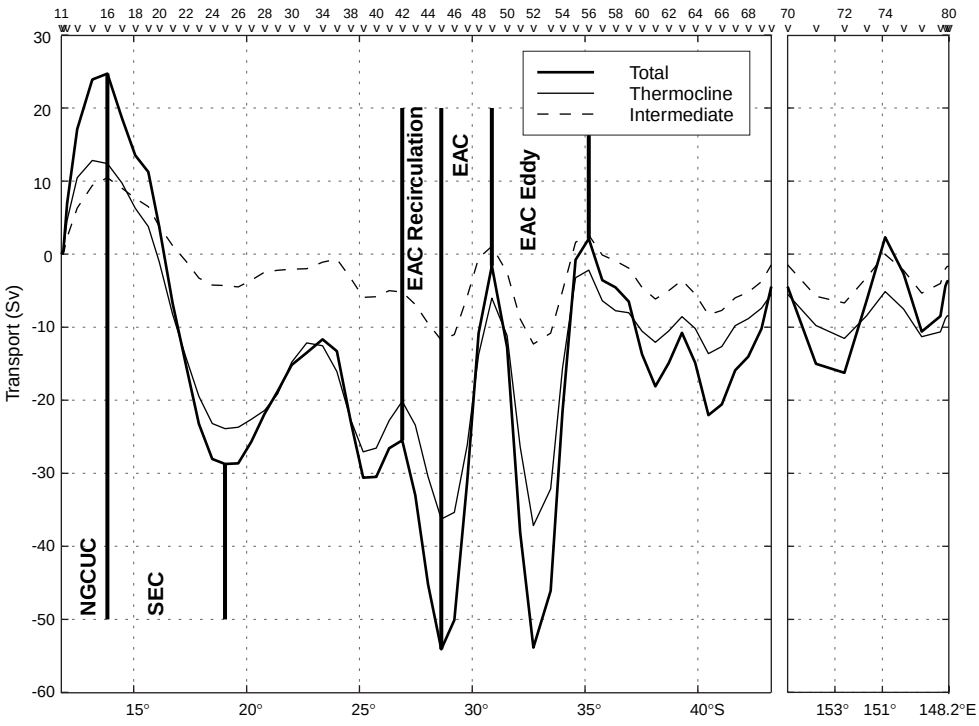

Figure 3. Transport (Sv) at WOCE section P11 accumulated southward from the Louisiade Archipelago.

At the northern end of P11 the subsurface flow of the NGCUC with current speeds as high as 55 cm/s is supplemented by the New Guinea Coastal Surface Current (NGCSC) which flows in the same direction with velocities up to 75 cm/s. A very narrow westward flowing counter-current is found adjacent to the coast. The net eastward transport of the combined NGCUC/NGCSC is 26.4 Sv.

The circulation field of the EAC

About half the inflow to the Coral Sea (29 Sv) flows south from the SEC bifurcation at 18°S to feed the EAC (assuming zero net transport through Torres Strait). Along the Australian coast the EAC forms a system of deep eddies reaching at least 2000 m depth with the main flow located along the continental slope (Figs. 2a, b). The uniformity of water mass characteristics along isopycnals south of Cato I. indicates that the current is continuous along the western boundary of the Tasman Sea, and that vigorous stirring by EAC eddies and meanders acts to homogenise water properties.

The EAC separates from the coast and crosses P11 near 30°S. The steeply sloping isotherms associated with the current persist from the surface to the bottom (Fig. 2a). The total geostrophic transport of the EAC after separation is 56.6 Sv (Fig. 3). The EAC transport and the total/upper 1300 m geostrophic transport ratio are consistent with results obtained by earlier studies.

After separating from the coast, one branch of the EAC recirculates to the north and then west, crossing P11 again at 28°S, while the remainder can be traced as a continuous meandering eastward jet crossing the Tasman Sea and lying at about 25–30°S between New Zealand and Fiji. The surface position of the Tasman Front, and the core of the EAC in the Tasman Sea, is well defined by the winter outcropping of the 20°C isotherm. Our estimate of the total top-to-bottom transport of the EAC is 57 Sv, where 33 Sv recirculates to the west, leaving a net outflow of 24 Sv.

A warm-core anticyclonic eddy is located south of the latitude where the EAC turns offshore (Figs. 2–3). The total transport of the eddy is 60 Sv (relative to the bottom), slightly in excess of the EAC transport. Like the EAC, the eddy extends from the surface to the sea floor, and at a depth of 1300 m the geostrophic velocities exceed 10 cm/s.

The circulation of the southern Tasman Sea

The circulation of the southern Tasman Sea is characterised by highly variable flows and a lack of strong mean currents. The maps by Wyrtki (1962) and Reid (1986) show that part of the EAC continues beyond the separation point as far south as Tasmania. Previous studies disagree as to whether this flow turns east (e.g. Wyrtki, 1962; Stramma et al., 1995) or west (e.g. Reid, 1986) on reaching the southern tip of Tasmania. Estimates of the net flow through the Tasman Sea between Tasmania and New Zealand also vary, although the consensus appears to be that there is a net flow to the south.

The flow at the southern end of P11 and the section at 43°S agrees well with the circulation patterns inferred from the water property distribution. Near the coast of Tasmania 15.3 Sv of subtropical water is carried southward across 43°S, some of which recirculates northward further east. The strongest inflow of water from the south occurs between 154°E and 155°E, where the thickest SAMW and freshest AAIW are found (Figs. 2a, b). After crossing the south-east corner of box defined by P11, this flow turns north and west to intersect the P11 section again at 37.5°S and 40°S (along with additional inflow across 43°S east of 155°E). These currents are presumably part of the anticyclonic cell south of Tasmania apparent in the dynamic topography by Reid (1986) and Davis (1998).

The net transport across P11 south of 30°S, where the EAC leaves the coast and crosses the section, is close to zero (Fig. 3). About 10.5 Sv of subsurface and intermediate waters from the subantarctic zone enter the region at the southern periphery of the anticyclonic cell, but most of this is returned to the south so that little SAMW and AAIW entering across 43°S continues northward through the Tasman Sea, consistent with the property distributions.

Circulation in density layers

Several authors have described the low latitude western Pacific as a "water mass cross-roads" where intergyre and interbasin exchange is enhanced (e.g. Fine et al., 1994; Schmitz, 1996). In particular, water from the South Pacific which feeds the Equatorial Undercurrent, the Indonesian Throughflow, and the North Pacific first passes through the Coral and Solomon Seas to reach the equator.

Our results confirm the continuity of a coastal undercurrent south of PNG, linking the GBRUC and the NGCUC flowing through Vitiaz Strait on the northern side of PNG. The total eastward flow is 26 Sv. Approximately half of this is relatively high oxygen water which enters the Coral Sea in the middle branch of the SEC near 16°S. The remainder is low oxygen water carried into the Coral Sea in the northern branch of the SEC.

Schmitz (1996) compared estimates of the transport in several layers across 32°S (based on the results of Toole et al., 1994) and through Vitiaz Strait (based on the results of Murray et al., 1995) and found that the flow leaving the basin was dominated by thermocline water, while the flow entering from the south was dominated by denser mode and intermediate waters. He hypothesised that the required conversion of dense to light water occurred in the Peru Current, although he did not have a lot of data to confirm this.

Our estimates of transport in the NGCUC south of PNG suggest that relatively little diapycnal conversion is required between 32°S and the northern Coral Sea. Wijffels et al. (1999) recently presented the revised geostrophic transport across WOCE section P6 constrained by ALACE float measurements of velocity at 900 m. They showed that 17.2 Sv of thermocline water with neutral density γ_n between 25.0 and 27.0 and 15.7 Sv of intermediate water

(γ_n = 27.0 – 27.7) enter from the south across 32°S east of the Kermadec Ridge. At P11 the SEC transported into the Coral Sea 15.3 Sv of intermediate water, 22.9 Sv of thermocline water, and about 13.9 Sv of lighter varieties (with γ_n less than 25.0) of surface waters not observed at P6. Within the uncertainty of both these estimates, the flows are similar and suggest that there is no need to convert a large volume of intermediate water to thermocline water within the subtropical Pacific north of 32°S.

About half the inflow of intermediate and thermocline waters to the Coral Sea (28.6 Sv) flows south from the SEC and feeds the EAC, and the other half (24.1 Sv) is carried by NGCUC into the Solomon Sea. A number of questions remain. Our net eastward flow south of PNG matches the combined directly measured flow through Vitiaz Strait (15.8 Sv) and estimated flow at St. George's Channel (about 8 Sv). However, the inflow of intermediate water (10.8 Sv) is larger than previous estimates of the transport in this layer through Vitiaz Strait (2.2 Sv, Murray et al., 1995; 2–4 Sv, Tsuchiya, 1991). But only a very thin layer of intermediate water is able to penetrate through the shallow Vitiaz Strait. Perhaps some intermediate water flows north through St. George's Channel or Solomon Strait, or there may be a local recirculation which carries some of this eastward flow back to the south to feed the northern branch of the SEC.

A more definitive statement regarding the intergyre exchange of intermediate water and the location of the diapycnal processes required to convert intermediate water to throughflow water awaits an analysis of the complete WOCE data set in the Pacific.

References

Boland, F. M., and B. V. Hamon, 1970: The East Australian Current, 1965–1968. Deep-Sea Res., 17, 777–794.

Davis, R., 1998: Preliminary results from directly measuring mid-depth circulation in the tropical and South Pacific. J. Geophys. Res., 103, 24619–24640.

Fine, R. A., R. Lukas, F. M. Bingham, M. J. Warner, and R. H. Gammon, 1994: The western equatorial Pacific: A water mass crossroads. J. Geophys. Res., 99(C12), 25063–25080.

Hamon, B. V., 1970: Western boundary currents in the South Pacific. In: Scientific Exploration of the South Pacific, W. S. Wooster, (ed.), pp. 51–59, US National Academy of Sciences.

Mulhearn, P. J., J. H. Filloux, F. E. M. Lilley, N. L. Bindoff, and I. J. Ferguson, 1988: Comparisons between surface, barotropic and abyssal flows during the passage of a warm-core ring. Aust. J. Mar. Freshwater Res., 39, 697–707.

Murray, S., E. Lindstrom, J. Kindle, and E. Weeks, 1995: Transport through the Vitiaz Strait. WOCE Notes, 7(1), 21–23.

Reid, J. L., 1986: On the total geostrophic circulation of the South Pacific Ocean: flow patterns, tracers and transports. Progr. Oceanogr., 16, 1-61.

Schmitz, W. J., Jr., 1996: On the world ocean circulation: Volume II. The Pacific and Indian Oceans/A global update. Technical Report WHOI-96-08, 237 pp., Woods Hole Oceanographic Institution, USA

Sokolov, S., and S. Rintoul, 1999: Circulation and water masses of the southwest Pacific: WOCE section P11, Papua New Guinea to Tasmania. J. Mar. Res., submitted.

Stramma, L., R. G. Peterson, and M. Tomczak, 1995: The South Pacific Current. J. Phys. Oceanogr., 25, 77-91.

Toole, J. M., S. E. Wijffels, M. S. McCartney, B. A. Warren, H. L. Bryden, and J. A. Church, 1994: WOCE hydrographic section P6 across the subtropical South Pacific Ocean. In: The Oceanographic Society, Pacific Basin Meeting, July 19–22, 1994, Honolulu, Hawaii, p. 76.

Tsuchiya, M., 1991: Flow path of the Antarctic Intermediate Water in the western equatorial South Pacific Ocean. Deep-Sea Res., 38, Suppl. 1, S273–S279.

Wijffels, S. E., J. M. Toole, and R. Davis, 1999: Revising the South Pacific subtropical circulation: a synthesis of WOCE observations along 32°S. J. Geophys. Res., submitted.

Wyrtki, K., 1962: Geopotential topographies and associated circulation in the western South Pacific Ocean. Aust. J. Mar. Freshwater Res., 13, 89–105.

JGOFS Open Science Conference, 13–17 April 2000

The Joint Global Ocean Flux Study (JGOFS) is a Core Project of the International Geosphere-Biosphere Programme (IGBP), and is jointly sponsored by the Scientific Committee on Oceanic Research (SCOR). JGOFS investigates the role played by ocean biogeochemical processes in the earth's carbon cycle. The project aims to assess and understand the processes controlling carbon exchanges between the atmosphere, ocean surface and ocean interior.

Since 1989, JGOFS has carried out biogeochemical process studies and other field campaigns in all ocean basins. The resulting data sets are unprecedented in both scope and accuracy, and have led to changes in our understanding of how ocean biogeochemical cycles function.

JGOFS is now entering a synthesis and modelling phase. As the efforts continue to develop 3-D global biogeochemical models, new challenges are emerging. Ultimately, the JGOFS synthesis goal is to improve process understanding and assimilate data sets into models for validation and enhance predictive capabilities.

The conference

The conference, titled "Ocean Biogeochemistry: A New Paradigm" focuses on the challenges of the JGOFS Synthesis and Modelling phase. The purpose of this conference is to provide an opportunity for scientists who are involved in the observational and modelling activities to present and discuss the results of JGOFS 10-year field programme to the broader ocean, atmosphere and terrestrial science communities. In addition, the conference aims to highlight the new and ongoing intellectual challenges that remain, in order to derive maximum benefit from the investment in JGOFS by national funding agencies.

Format and themes

The Conference format will consist of keynote talks on ocean biogeochemical themes, discussion sessions, and contributed papers and posters on the following themes:

- Ocean Biogeochemical Regimes: Hugh Ducklow, Virginia Institute of Marine Sciences, US.
- Carbon Dioxide Flux: Andrew Watson, University of East Anglia, UK.
- Regional and Global Primary Production: Paul Falkowski, Rutgers University, US.
- Continental Margins: Arthur Chen, National Sun Yat-Sen University, Taiwan.
- Community Structure: Michael Landry, University of Hawaii, US.
- Water Column Biogeochemistry: Paul Tréguer, Université de Bretagne Occidentale, France.
- Deep Ocean Fluxes: Karin Lochte, Institut für Ostseeforschung, Germany.
- Temporal Variability of Biogeochemistry: (to be announced).
- Ocean Carbon and Ecosystem Modelling: Scott Doney, National Center for Atmospheric Research, US.
- Feedback Processes: Philip Boyd, National Institute for Water and Atmosphere, New Zealand.

Young scientists are encouraged to present JGOFS work.

The venue

The conference will be held in Bergen, the former Viking Capital of Norway. Bergen is worth a visit and always has something to offer – no matter what time of year. It is an international town full of history and tradition: a big town with small-town charm and atmosphere. Visit the Medieval Fort and residence "Håkons Hall" and then wander along the wharf "Bryggen" with its unique architecture of pointed gables. UNESCO lists this maze of wooden buildings as one of the world's most significant examples of the history and culture of a medieval settlement. To get a good view of the city take the Funicular to the top of Mount Fløyen (320 m a.s.l.) or the cable car to Mount Ulriken (642 m a.s.l.) to see even more. Visit the famous fish market and taste Norwegian specialities such as smoked salmon or shrimps.

Bergen is the gateway to one of the world's most spectacular tourist attractions – The Norwegian Fjords. There are plenty of tours in and around Bergen to provide you with unforgettable memories. The conference agent PLUS Convention Norway will present options for travel within Norway and will be happy to answer any questions as well as make reservations.

Social events

Opportunities will be provided for informal discussions away from the conference. Several social events and excursions are being planned but some free time will also be available. Participants may want to take advantage of the exciting events in music, fine arts, dance and theatre that will be taking place at the time of their stay. Bergen has been chosen as one of the cities in Europe to represent culture in 2000, and there is expected to be a program with something of interest for everyone.

Second announcement

The Second Announcement will be printed later this year. Further details concerning the programme, accommodation, and other relevant information will be available at that time.

Committees

Conference Organisers:
Michael Fasham, Southampton Oceanography Centre, UK.; Roger Hanson, International Project Office (IPO), Bergen; and Karin Lochte, Institut fur Ostseeforschung.

Science Programme Committee:
Véronique Garçon, Centre National de la Recherche Scientifique, France; Kon-Kee Liu, National Taiwan University; Graham Shimmield, Dunstaffnage Marine Laboratory, Scotland; Toshiro Saino, Nagoya University, Japan; and Ulf Lie, University of Bergen, Norway.

Local Norwegian Committee:
Roger Hanson and Beatriz Baliño, IPO; Ulf Lie, Truls Johannessen and Dag Aksnes, University of Bergen.

Conference arrangements:
PLUS Convention AS and Judith Stokke, IPO.

Sponsors

The conference is sponsored through the Scientific Committee on Oceanic Research (SCOR), and the International Geosphere-Biosphere Programme (IGBP). The conference will also be organised in association with the University of Bergen (UiB), the Research Council of Norway (NRC), and the Center for Studies of Environment and Resources (SMR/UiB).

Conference web site

The official JGOFS Conference web site may be found at the following URL:

http://ads.smr.uib.no/jgofs/conference.htm

Here you will find information about the Scientific programme such as details of the keynote lectures, poster submission and accommodation options.

Presentations

The call for papers and posters (abstracts) will be made in later this year with a submission deadline of 1 October 1999. A book of abstracts will be produced prior to the meeting.

Accommodation

Reservations have been made at the Bergen Hotel, which is part of the Bergen Congress Center where the conference will be held. In addition, alternative accommodation has also been arranged for the low-budget traveller.

Travel and support

Bergen is regarded as an international congress city, with good internal and international air connections as well as train connections from Oslo. Delegates must make their own reservations to Norway.

Limited funding might be available to support the participation of students. An indication of whether you may require support should be made at the time of initial registration.

Enquiries

Enquiries regarding the scientific programme should be directed to:

JGOFS International Project Office, SMR/UiB, High Technology Center, 5020 Bergen, Norway. Tel: +47 5558 4244 Fax: +47 5558 9687. E-mail: Roger.Hanson@jgofs.uib.no URL: http://ads.smr.uib.no/jgofs/jgofs.htm

Travel enquiries within Norway should be directed to:

PLUS Convention Norway, C. Sundtsgt. 10, N-5004 Bergen, Norway. Tel: +47 55 54 40 40 Fax: +47 55 54 40 44 E-mail: bsb@plus-convention.no, URL: http://www.plus-convention.no/

Surface Ocean Lower Atmosphere Study (SOLAS) Open Science Conference (20–24 February 2000)

R. A. Duce (rduce@ocean.tamu.edu) and P. S. Liss (p.liss@uea.ac.uk), Co-Chairs, SOLAS Planning Committee

SOLAS is a potential new interdisciplinary research project whose planning to date has been sponsored by SCOR and IGBP with considerable interest from WCRP. The scientific focus for the proposed project is the interaction between the atmosphere, climate, and marine biogeochemical processes. SOLAS would benefit from the work of several previous programmes principally IGAC, JGOFS and WOCE and would be linked to CLIVAR. More information on the SOLAS programme can be found at:

http://www.ifm.uni-kiel.de/ch/solas/main.html

The purpose of the SOLAS Open Science Conference is to communicate and discuss the following and other related ideas with as wide a group of interested international scientists as possible.

The conference will be organised around a set of scientific questions to be presented in plenary talks and reviewed in discussion groups. Other topics have been chosen as well for presentations and discussion groups, mostly reviewing current skills and projected needs and capabilities for investigating ocean-atmosphere interactions. Plenary speakers and topics are:

- Meinrat Andreae, Max Planck Institut für Chemie, Mainz, Germany: How much might marine biological sulphur emissions change, and would such changes have climatic implications?
- Richard Barber, Duke University Marine Laboratory, US: How much might the atmospheric delivery of marine nutrients, such as iron and nitrogen, change, and would such changes have global implications?
- Andy Watson, University of East Anglia, UK: Are changes in marine biogeochemistry in the next century likely to have a significant influence on the net oceanic uptake of carbon dioxide?
- Scott Doney, National Center for Atmospheric Research, Boulder, US: Physical perspectives on how changes in climate-driven physical forcing might affect upper ocean biogeochemistry and air-sea fluxes.
- Peter Liss, University of East Anglia, UK: Biogeochemical perspectives on how changes in climate-driven physical forcing might affect upper ocean biogeochemistry and air-sea fluxes.
- Barry Huebert, University of Hawaii, US: Are changes in the marine emissions of gases and particles likely to have a significant influence on atmospheric chemistry?
- Neil Blough, University of Maryland, US: Are changes in the spectrum and intensity of radiation likely to affect the production of trace gases in the surface ocean?

Poster sessions are also planned, further details to be announced.

The conference will be hosted by the Institut für Meereskunde in Kiel, Germany, and will be held in Damp, which is a resort village and conference centre on the Baltic coast just north of Kiel. A registration fee of DM190 (approx. US$100) is requested (non-refundable after 8 October 1999). For accompanying family members, friends, etc. who wish to attend conference social activities, etc. but not the actual meeting, a reduced fee of DM80 (US$40) will be charged. Some funds are being sought to cover some travel costs for this meeting. However this support will be very limited and is designed to encourage attendance of younger scientists and those from developing countries.

Damp can be reached by flights to Hamburg, or Kiel (via Frankfurt). Bus transfers will be arranged. Accommodation costs at Damp will be approximately DM140 per night, which includes breakfast. Lunch and Dinner can be expected to cost up to an additional DM50 per day, although several receptions and lunch buffets during the meeting will be hosted.

Further conference information is available at:

http://www.ifm.uni-kiel.de/ch/solas/meeting.html

Downloadable files of the conference registration form with full instructions can also be obtained from this site.

Enquiries about the conference or registration procedure can be directed towards the local host for the SOLAS Open Science Meeting:

Ute Weidinger - Conference Organizer
Institut für Meereskunde
Düsternbrooker Weg 20
24105 Kiel
Germany
Phone/Fax: +49 (431) 597 3811
e-mail: solas@ifm.uni-kiel.de.

Atlas of Ocean Sections CD-ROM

V. Gouretski and K. Jancke, WHP SAC, Hamburg, Germany; J. Reid and J. Swift, Scripps Institution of Oceanography, La Jolla, USA; P. Rhines, University of Washington, Seattle, USA; R. Schlitzer, AWI, Bremerhaven, Germany; I. Yashayaev, BIO Dartmouth, Canada. jswift@ucsd.edu

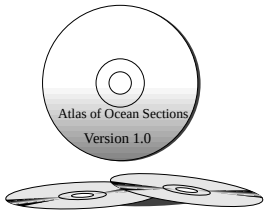

Version 1 of the Atlas of Ocean Sections CD-ROM is now available. Contents include 2120 sections assembled from the original NODC data files contributing to Joe Reid's World Ocean data collection, with corrections to many of the data for known offsets (mostly standard seawater batch offsets) and many of the obvious bad data values culled. The sections are available on the CD in NODC SD2 standard data exchange format (an ASCII format) and also in OceanAtlas binary (Mac OS, and, soon, Java OceanAtlas) and Ocean Data View binary (Windows 9X and NT). The sections are indexed by region, ship name, and year, and are accessed either via an included browser interface or by copying files.

Also on the CD are the applications ATLAST (PC/MS-DOS), Ocean Data View (PC/Windows 9X & NT), and Power OceanAtlas (Mac OS), plus a Northwest Atlantic Atlas and a corrected World Ocean data set. There are also collections of WOCE bottle data and Arctic CTD & bottle data in OceanAtlas binary format.

Version 1 of the AOS CD-ROM is directed primarily at professional oceanographers. The upcoming Version 2 promises to be easier to use, and aimed at both educational and professional users.

The OceanAtlas project, including the Atlas of Ocean Sections, has been supported principally by NSF, with additional support from NOAA. Distribution is supported by NASA.

The CD-ROM is free and is available only from: http://podaac.jpl.nasa.gov/order/order_displaytools.html.

Nearly all Atlas of Ocean Sections materials are also available by download from the OceanAtlas web site (http://odf.ucsd.edu/OceanAtlas), which also includes beta versions of the new Java OceanAtlas application, which will (soon) run on Windows (9X & NT), Mac OS, and Unix. (Installers for Windows and Unix should be available from 7/1999.) Java OceanAtlas on any platform will directly open the OceanAtlas binary data files on the Atlas of Ocean Sections CD-ROM.

For additional information contact:

Jim Swift
Isaacs Hall (NORPAX)
Room 305
Tel. 1-858-534-3387
jswift@ucsd.edu

MEETING TIMETABLE 1999/2000

1999		
October 4–8	WOCE-26 Meeting	La Jolla, USA
October 18–22	The Ocean Observing System for Climate	S. Raphael, France
October 25–27	Topex/Poseidon/Jason-1 SWT	S. Raphael, France
December 13–17	AGU Fall Meeting	S. Francisco, USA
2000		
January 24–28	AGU Ocean Sciences Meeting	S. Antonio, USA
February 20–24	SOLAS Open Science Conference	Kiel, Germany
March 13–17	JSC Annual Meeting	Tokyo, Japan
April 3–7	Southern Hemisphere Meteorology and Oceanography	Santiago de Chile, Chile
April 13–17	JGOFS 2nd Open Science Conference "Ocean Biogeochemistry: A New Paradigm"	Bergen, Norway
April 25–29	EGS General Assembly	Nice, France
May 1–5	CLIVAR SSG 9th Session	Honolulu, USA
May 30–June 3	AGU Spring Meeting	Washington, USA
June 27–30	2000 Western Pacific Geophysics Meeting	Tokyo, Japan
December 15–19	AGU Fall Meeting	S. Francisco, USA

The WOCE International Newsletter is published by the WOCE International Project Office.

Editor:
Roberta Boscolo

Compilation and layout:
Sheelagh Collyer

The International WOCE Newsletter is distributed free-of-charge upon request thanks to the funding contributions from France, Japan, UK, and WCRP.

This Newsletter provides a means of rapid reporting of work in progress related to the Goals of WOCE as described in the WOCE Scientific and Implementation Plan.

Requests to be added to the mailing list and changes of address should be sent to:
WOCE IPO
Southampton Oceanography Centre
Empress Dock
Southampton SO14 3ZH
United Kingdom
Tel. +44 23 8059 6205
Fax. +44 23 8059 6204
e-mail: woceipo@soc.soton.ac.uk

Contents of past issues together with the electronic PDF version can be found at:
http://www.soc.soton.ac.uk/OTHERS/woceipo/acrobat.html

Articles, letters, announcements and reviews are welcome and should be addressed to the editor.

Printed by Technart Ltd.
Southern Road
Southampton SO15 1HG
United Kingdom.

If undelivered please return to:

WOCE IPO
Southampton Oceanography Centre
Empress Dock
Southampton SO14 3ZH
United Kingdom.

CONTENTS OF THIS ISSUE